



Radar Systems and  
Remote Sensing Laboratory

AD-A276 568



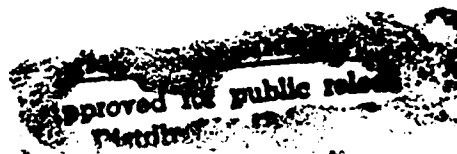
SCATTEROMETER WIND-SPEED EXPONENTS:  
A REVIEW AND SAXON 35-GHZ MEASUREMENTS

DTIC  
ELECTE  
MAR 09 1994  
S E D

DTIC QUALITY INSPECTED 2

THE UNIVERSITY OF KANSAS CENTER FOR RESEARCH, INC.

2291 Irving Hill Road  
Lawrence, Kansas 66045-2969



12

**SCATTEROMETER WIND-SPEED EXPONENTS:  
A REVIEW AND SAXON 35-GHZ MEASUREMENTS**

Xiaoping Wang

DTIC  
SELECTED  
MAR 09 1994  
S E D

Radar Systems and Remote Sensing Laboratory  
Department of Electrical Engineering and Computer Science, University of Kansas  
2291 Irving Hill Road, Lawrence, Kansas 66045-2969  
TEL: 913/864-4835 \* FAX: 913/864-7789 \* OMNET: KANSAS.U.RSL

RSL Technical Report 8621-2

August 1993

Sponsored by:

Office of Naval Research  
Arlington VA 22217-5000

Grant N00014-89-J-3221

Approved for public release  
Distribution is unlimited

Accession For	
NTIS CRA&I	<input checked="" type="checkbox"/>
DTIC TAB	<input type="checkbox"/>
Unannounced	<input type="checkbox"/>
Justification	
By	
Distribution /	
Availability Codes	
Dist	Avail and/or Special
A-1	

94-05325



4 2 17 047

## TABLE OF CONTENTS

	PAGE
ACKNOWLEDGEMENTS	
ABSTRACT.....	
LIST OF FIGURES.....	
1. INTRODUCTION	
1-1. History of experiments for ocean wind (after 1985).	
1-2. Background of SAXON experiment.	
2. PRINCIPLE OF WINDSPEED EXPONENT MEASUREMENT	
2-1. Linear Regression Methods	
(ordinary linear regression and orthogonal linear regression)	
2-2. Measurement Errors	
(both wind speed and radar noise.)	
3. WINDSPEED EXPONENT MEASUREMENT IN SAXON	
3-1. Power measurement	
(calculation of mean power from the three beams)	
3-2. Data classification	
(upwind and crosswind)	
3-3. Results	
A. with the data of wind direction and wave direction are same.(OR and OLR are almost same)	
B. with the data of wind direction and wave direction are different.(OR is higher than OLR)	

#### **4. VARIATION OF WIND EXPONENT WITH ANGLE OF INCIDENCE**

##### **4-1. Derivation of Bilinear Regression**

##### **4-2. Discussion**

#### **5. CONCLUSION AND SUGGESTIONS**

#### **6. REFERENCES**

## List of Figures

Numbers	Figure Description
Figure 1-1	Example of circle-flight observations
Figure 1-2	Comparison of AAFE Radscat 13.9 GHz $\sigma^0$ measurements with theory of Chan and Fung (1977)
Figure 1-3	(a) Regression fit for Skylab $\sigma^0$ measurements at $32^\circ$ angle of incidence (b) Regression fit for Skylab $\sigma^0$ measurements at $1^\circ$ angle of incidence.
Figure 1-4	Tower-based measurements of the wind speed response of scattering at 10 GHz.
Figure 1-5	Upwind speed response exponents from different experiments.
Figure 1-6	Downwind speed response exponents from different experiments.
Figure 1-7	Crosswind speed response exponents from different experiments.
Figure 1-8	(a) The range of windspeed in SAXON-FPN during November, 1990. (b) The range of wind direction in SAXON-FPN during November, 1990.
Figure 2-1	Linked hodographs of velocity vectors in oceanic and atmospheric PBLs.
Figure 3-1	(a) Diagram of SAXON-FPN (b) Radar look direction and ambiguous region.
Figure 3-2	Configuration of the Vector Slope Gauge System.
Figure 3-3	Regions of different wave or wind direction.
Figure 3-4	The range of wind conditions encountered from 19 to 23 November. (a) Wind speed vs day (b) Wind direction vs day
Figure 3-5	Upwind speed response exponent under both Up and Crosswave conditions.

Figure 3-6 Upwind speed response exponent under Crosswave condition.

Figure 3-7 Crosswind exponent under both Up and Crosswave conditions.

Figure 3-8 Crosswind exponent under Upwave condition

Figure 4-1 Bilinear regression for Upwind under VV polarization.

Figure 4-2 Bilinear regression for Downwind under VV polarization.

Figure 4-3 Bilinear regression for Upwind under HH polarization.

Figure 4-4 Bilinear regression for Downwind under HH polarization.

## ABSTRACT

Most studies of upper ocean circulation, tropospheric dynamics, and air-sea interaction require the measurement of near-surface vector winds over the oceans under all-weather conditions. Radar scatterometers may be used to find the surface wind vector. The scattering coefficient of the ocean usually is assumed to take the form

$$\sigma^0 = A u^\gamma$$

where  $u$  is the wind speed.

To determine the correct wind exponent  $\gamma$  by microwave scatterometers is therefore very important. Many experiments on scattering from the oceans provide similar but different values of  $\gamma$ .

Most experimenters apply the ordinary least-square regression (OLR) to extract  $\gamma$  from measurements. However, this technique assumes that only one variable may be in error, so such a result may not be statistically correct. As an alternative, orthogonal regression (OR) provides the best results when both variables have similar scales. The wind exponent  $\gamma$  is discussed in two cases with both OR and OLR. Case one is when both wind direction and wave direction are same, in the Up direction, and case two when the two direction are orthogonal. For case one, OR and OLR were found to have close results; however results are quite different for the second case.

It is necessary to find optimum values of  $\gamma$  at different incident angles and directions. The optimum  $\gamma$  can be used to obtain the ocean surface windspeed. The bilinear regression described in the report is a simple but effective way to show the relation between  $\gamma$  and incidence angles. Results using OR provided a very good fit to the bilinear regression analysis of various experimental data.



## CHAPTER ONE

### INTRODUCTION

#### 1-1. History of experiments for radar ocean wind measurements (1968--).

The concept of inverting radar scattering amplitudes to determine the speed of the ocean surface winds using a scatterometer was proposed by Moore and Pierson in 1966 [1](Moore, R.K, W.J.Pierson,Jr. 1966). Since then many experiments have been conducted to determine the radar response under varying wave and wind conditions, and the theory of radar return from the sea has advanced significantly.

One of the most extensive experimental programs was initiated during the 1950s by the U.S. Naval Research Laboratory. This program conducted experiments using a multi-frequency airborne radar during a variety of sea conditions and at various radar look angles. The results of the 1950s experiments were reported in [2](MacDonald, 1956).

During the 1960s, the Naval Research Laboratory (NRL) continued the extensive aircraft measurements program to provide quantitative information on the parametric behavior of the electromagnetic scattering coefficient (RCS)  $\sigma^0$  of the ocean. Measurements were obtained as a function of polarization, incidence angle, and azimuth angle using 4-frequency pulse radars operating at 0.4, 1.2, 3(1950s), 4.4(1960s) and 9.0 GHz. Other aircraft measurements were later

performed by NASA, New York University and The University of Kansas using a NASA Johnson Space Center radar scatterometer at 13.3 GHz ( a fan-beam Doppler radar). Analysis of NASA observations at 13.3 GHz and NRL observations at 8.9 GHz and 4.4 GHz show the variability with wind speed. A detailed analysis is given in [3](Claassen, Moore, 1972). The NASA-JSC data sets were used to propose a microwave scatterometer technique for remotely sensing surface windspeed over the ocean.

More detailed correspondence between microwave scatterometer backscatter cross-section,  $\sigma^0$ , and measured surface wind was established in the 1970s using an airborne scatterometer flying near buoys and ships. This was extended to satellite data when NASA launched Skylab in 1973 and SEASAT in 1978. During this decade, the main experiments were:

\* AAFE program: An aircraft microwave scatterometer was developed at NASA Langley Research Center under the Advanced Applications Flight Experiments (AAFE) program. These experiments evaluated the viability of radar remote sensing of the surface wind vector(both speed and direction) using a circle flight experimental technique suggested by Jones. The results are shown in Fig.1-1, and 1-2 [4](Ulaby, F.T., Moore,R.K.,Fung,A.K.,1986).

\*Skylab Measurements: SKYLAB, launched in 1973, provided the first opportunity to observe the oceans from space. The SKYLAB S-193 instrument contained a radar scatterometer / radiometer at 13.9 GHz and a radar altimeter at the same frequency. With the great speed and vast coverage of a spaceborne instrument, only a few days observations were more than all the

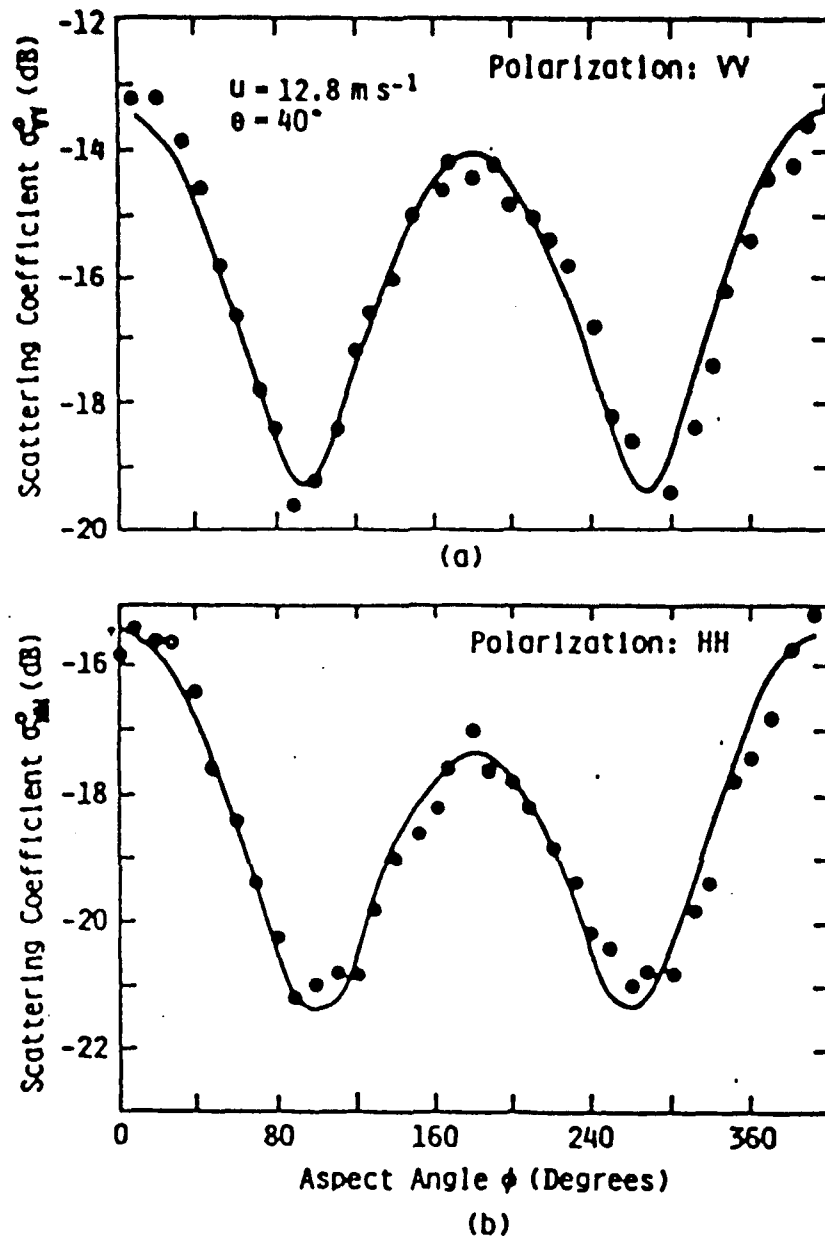


Figure 1-1 Example of circle-flight observations of the azimuthal variation of  $\sigma^0$  at 13. GHz, along with a regression line of the form of Eq. 11.46 (from Moore, *et al.*, 1978).  $\phi = 0$  corresponds to the upwind direction.

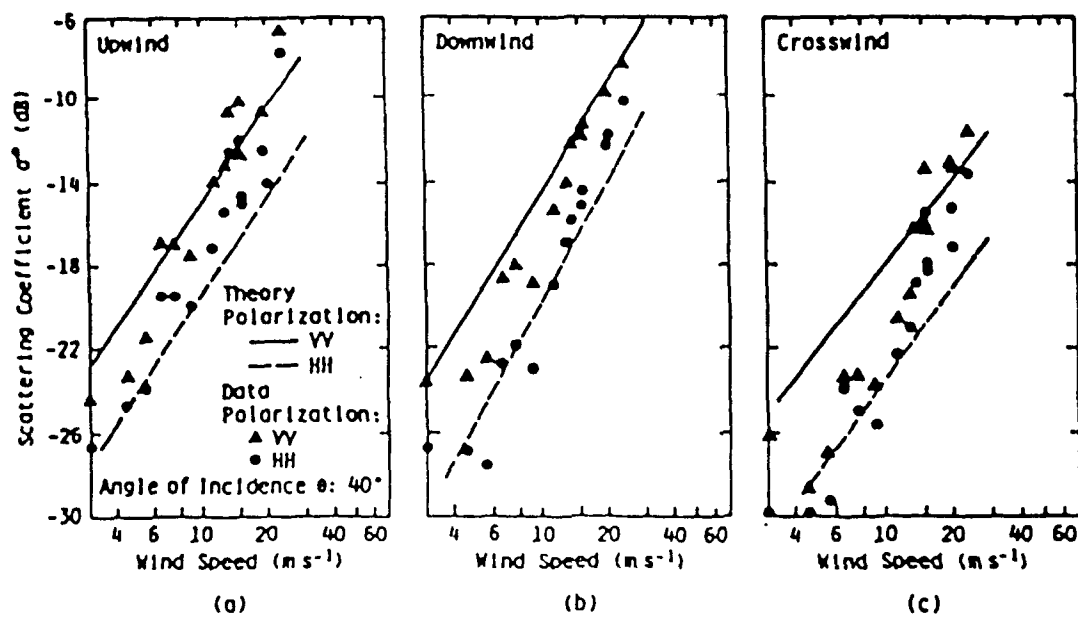


Figure 1-2 Comparison of AAFE Radscat 13.9 GHz  $\sigma^0$  measurements with theory of Chan and Fung (1977) (from Moore, *et al.*, 1978).

preceding programs combined [5]-[10]. However, since the spacecraft moves so fast and the time available for this particular experiment in the complex of SKYLAB experiments was limited, very few points were obtained where "surface-truth" wind measurements were available from the surface. Comparison of Skylab data with an underflight by the AAFE Radscat instrument showed they were within about 0.5 dB of each other. Comparison was also made with objective analyses of reports sent in by 900 ships on the North Atlantic. The ship measurements are not very reliable, but the results at least show that the value of  $\sigma^0$  increases with wind speed at incidence angles larger than 10 degrees, but decreases at vertical incidence. See Fig.1-3 and 1-4. [4] (R.K.Moore vol.iii))

\*Seasat Measurements of Ocean Backscattering: The SEASAT-A satellite was launched in June 1978. The goal was to develop meteorological and oceanographic measurements from space with microwaves. The measurement lasted only 99 days, but it provided reliable scatterometer data and SAR imagery under a variety of wind and wave conditions. To compare measurements made by SEASAT sensors with contemporaneous surface observations from a number of research vessels and moored buoys, two major experiments involving extensive surface measurements were conducted: the GOASEX experiment in the Gulf of Alaska, and the JASIN experiment in the North Atlantic between the British Isles and Iceland. The details of the two campaigns were presented in special issues of JGR, 1982; and JGR, 1983. The results show that the measurements of wind exponents from SEASAT are comparable with the previous aircraft experiments and Skylab campaign [Fig.1-5,1-6, and 1-7] [4](RKM, Vol iii)].

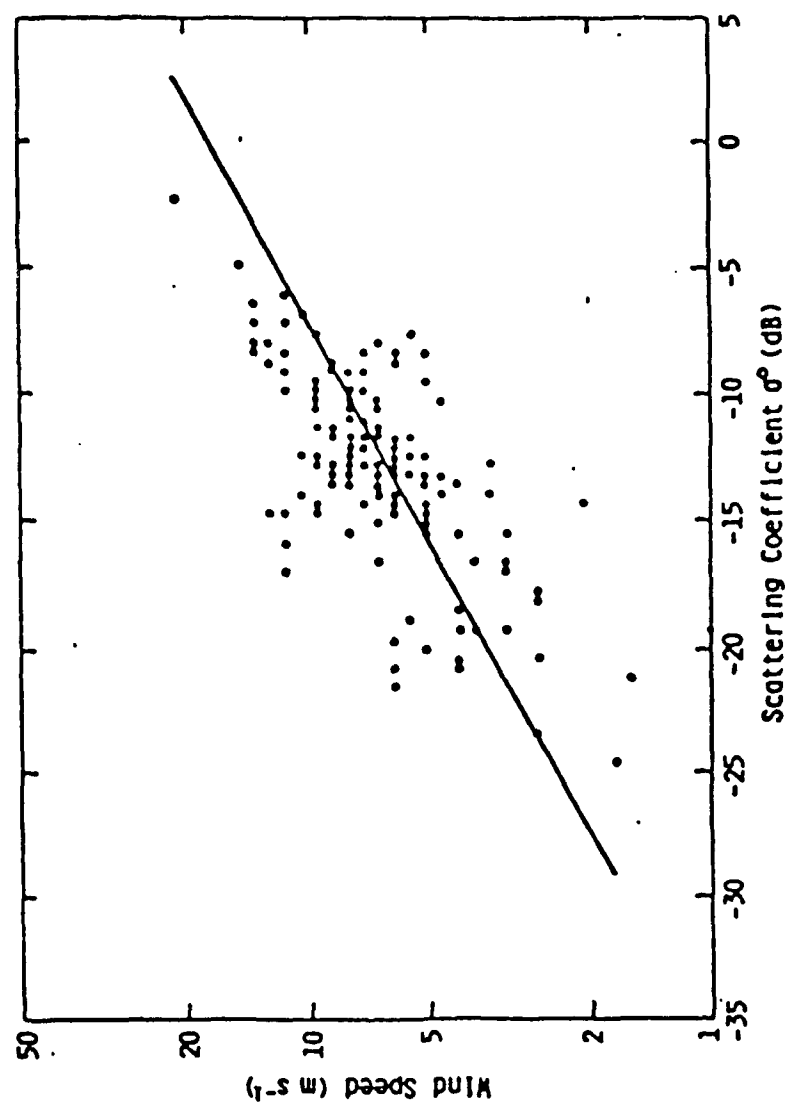


Figure 1-3(a) Regression fit for Skylab  $\sigma^0$  measurements at 32° angle of incidence (from Moore and Young, 1977).

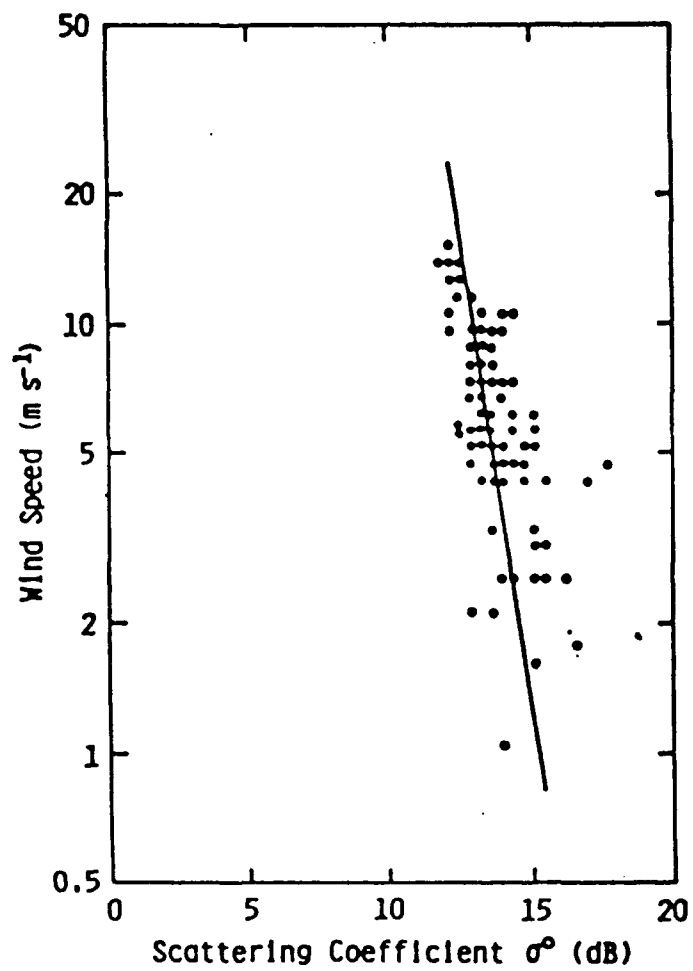


Figure 1-3 (b) Regression fit for Skylab  $\sigma^0$  measurements at 1° angle of incidence.

(from Moore and Young, 1977).

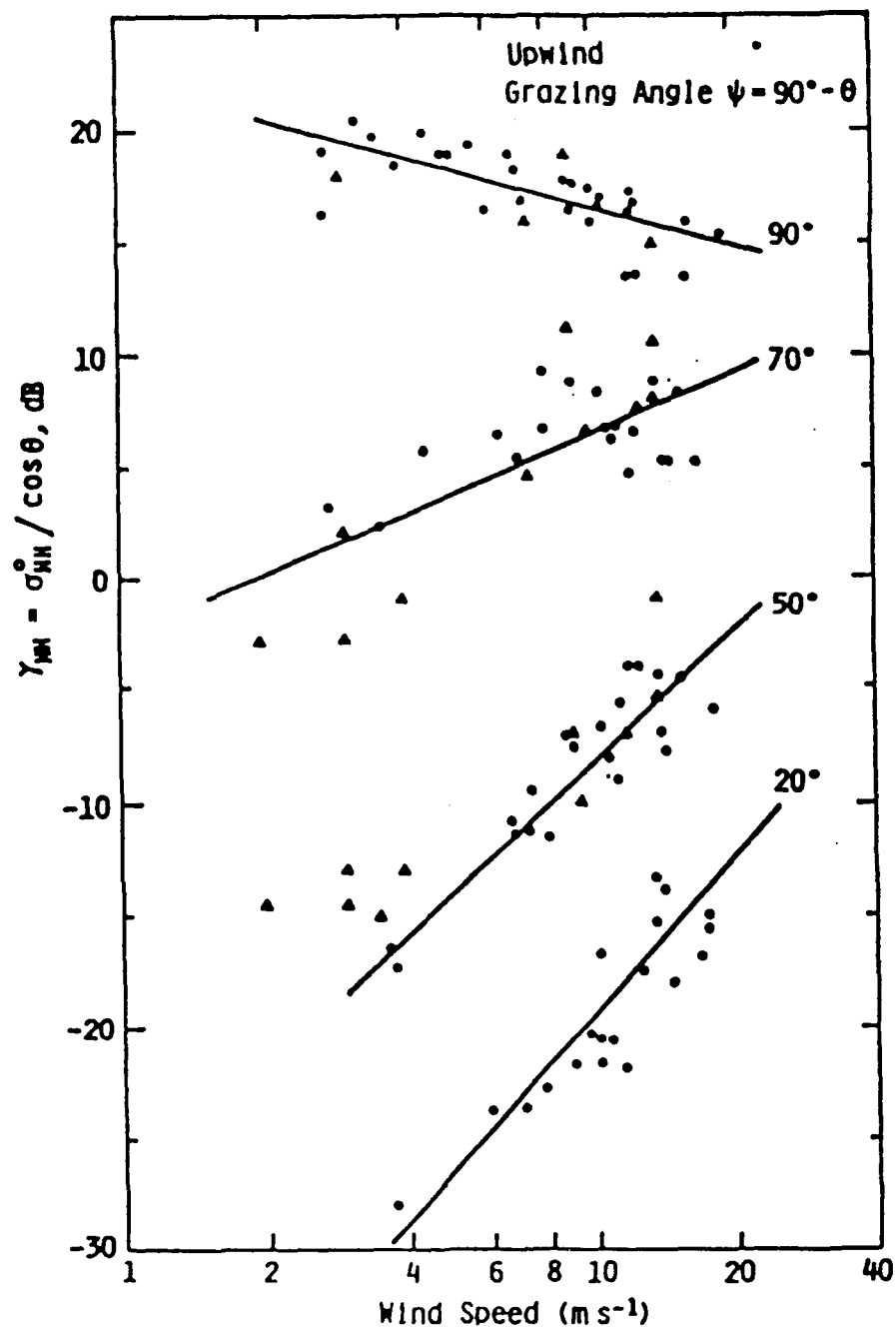


Figure 1-4 Tower-based measurements of the wind speed response of scattering at 10 GHz. Note that  $\gamma = \sigma^0 / \cos \theta$  is recorded, and that the angles given are the *grazing angles*, i.e., the complements of the incidence angles (from de Loor and Hoogeboom, 1983).



In the 1980s no spaceborne scatterometer flew, but there were many airborne campaigns. In this period the major experiments were:

TOSCANE campaign by IFREMER began in 1983: The purpose was to study the structure of ocean surface wind and to develop an array of instrumented buoys to be deployed at sea during the post calibration phase of the ERS-1 C-band wind scatterometer. The first campaign named PROMESS/TOSCANE I was conducted over the Atlantic ocean close to Brest, France, in 1984. It dealt with ship wind measurements and with airborne scatterometer calibration. In 1985 (from Feb. 14 to April 17), a second campaign called TOSCANE was performed near southern Brittany in France. The goal of the campaign was to compare the aircraft scatterometer data to data from an array of well-calibrated buoys for the ERS-1 satellite wind scatterometer calibration. To estimate the performance of the planned ERS-1 C- band VV polarization wind scatterometer, several airborne scatterometer measurements were carried out in the ESA'S Earth observation program with the multifrequency air-borne scatterometer DUTSCAT in the TOSCANE T campaign in 1987. Long developed a scattering model, CMOD1, using the DUTSCAT signature of the ocean database, [11] (Unal, C.M.H. et al.,1991) and [12] (Daniault, N.,1988).

FASINEX: From winter of 1985 to spring of 1986, the Frontal Air-Sea Interaction Experiment (FASINEX) was conducted in the subtropical convergence zone southwest of Bermuda. The goal of the experiment was more understanding of the relationships between radar backscatter from the ocean surface and the parameters of geophysical theory, which include the ocean wind stress, air-sea temperature difference, and sea-surface wave spectrum. In the experiment, the

observations and measurements were performed by buoys, ships, aircraft and spacecraft. Most of the data of the NASA Jet Propulsion Laboratory Active Microwave Scatterometer (AMSCAT) came from 10 measurement flights by the C130 aircraft. The AMSCAT operated at Ku band. For each measurement, the aircraft traveled 12km along a straight flight path at 1100 m altitude. The radar incidence angle was from 0 to 60 deg. and the azimuthal scan was about 330 deg. The ocean surface wind varied from 2 to 20 m/s. The total time of data collected was 30 hours [13] (Weissman, D.E, 1990) and [14](Plant, W.J.,1990)

NORCSEX: In March 1988, an ERS-1 prelaunch experiment on the Norwegian Continental Shelf (NORCSEX) was conducted. The basic objective of the experiment was to investigate the imaging capability of SAR on the ocean current surface. A secondary objective of NORCSEX was to assess the capability of a C-band SAR to measure ocean surface wind and waves. As the most critical parameter for remote sensing (SAR and scatterometer), the wind stress was measured by buoys and ships during NORCSEX.[15],[16],[17].

TOWARD: The Tower Ocean Wave and Radar Dependence Experiment was conducted from October 1984 to January 1986 at the Naval Ocean Systems Center Tower, located offshore of Mission Beach, San Diego, California. The general goal of the experiment was to provide an experimental basis to resolve the conflicting theories on synthetic-aperture radar (SAR) imaging of the ocean surface. The specific objectives stated for the TOWARD experiment included (1) investigation of the hydrodynamics of short waves and their modulation by long waves, (2) assessment of the assumptions stipulated in radar backscatter theory that are used in SAR

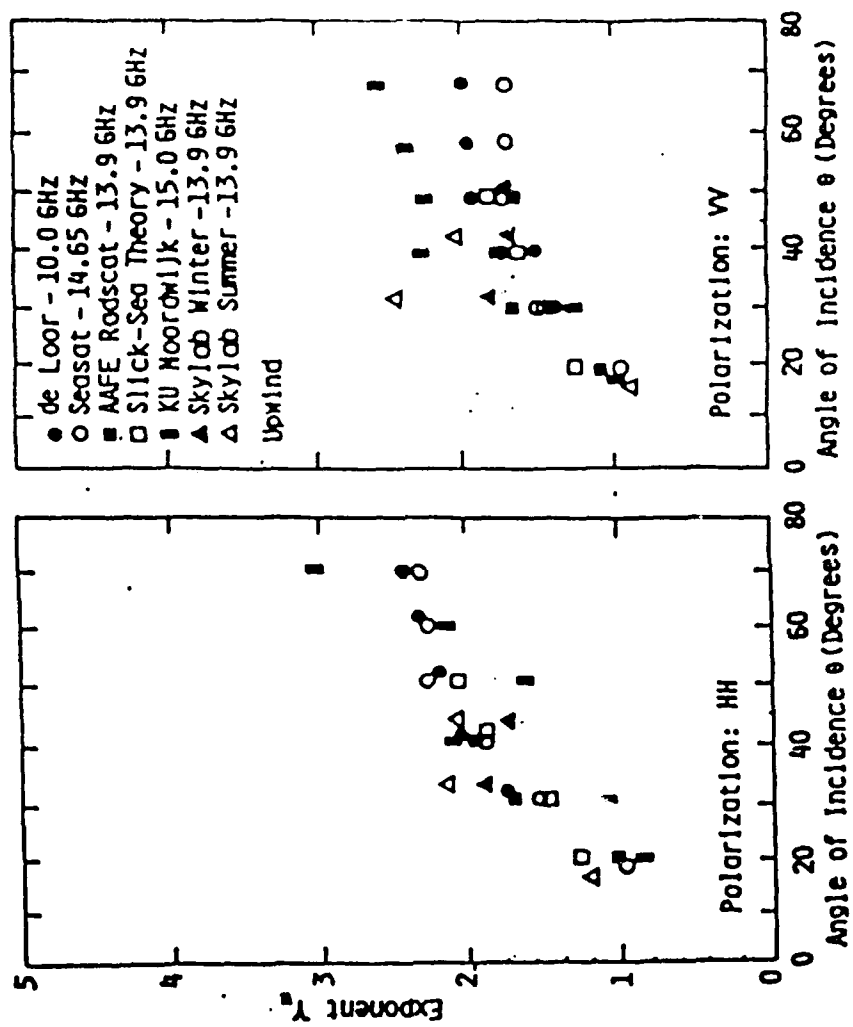


Figure 1-5 Upwind speed response exponents from different experiments.

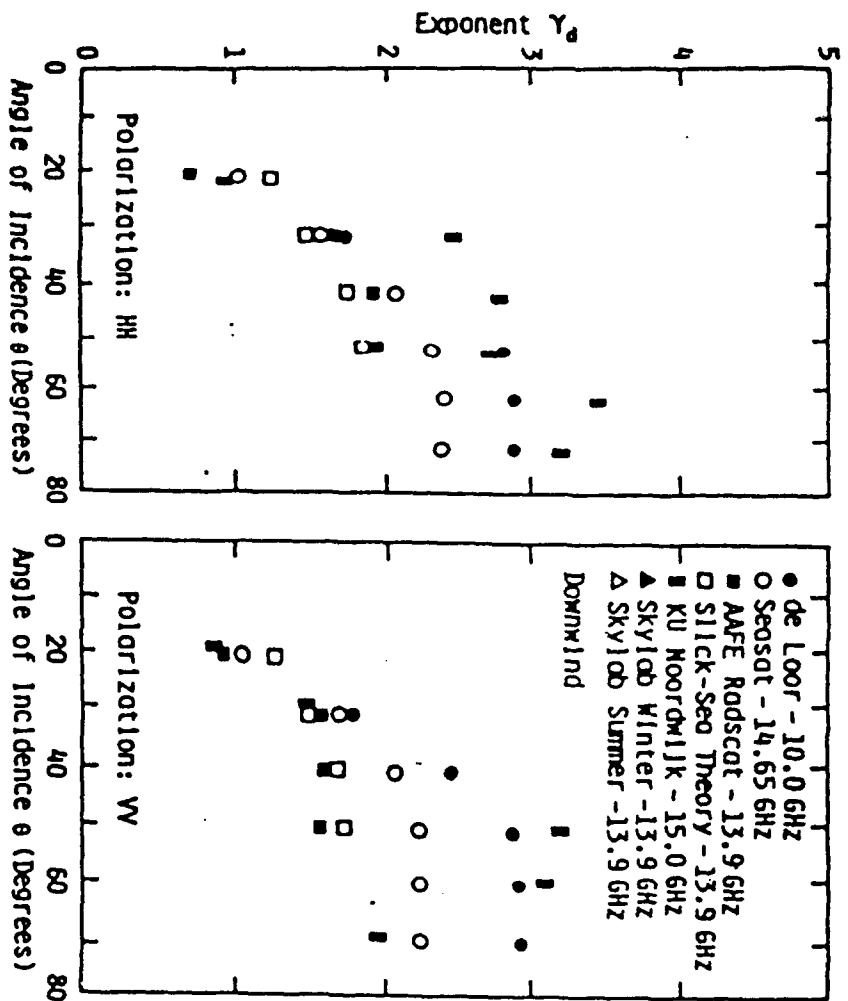


Figure 1-6 Downwind speed response exponents from different experiments.

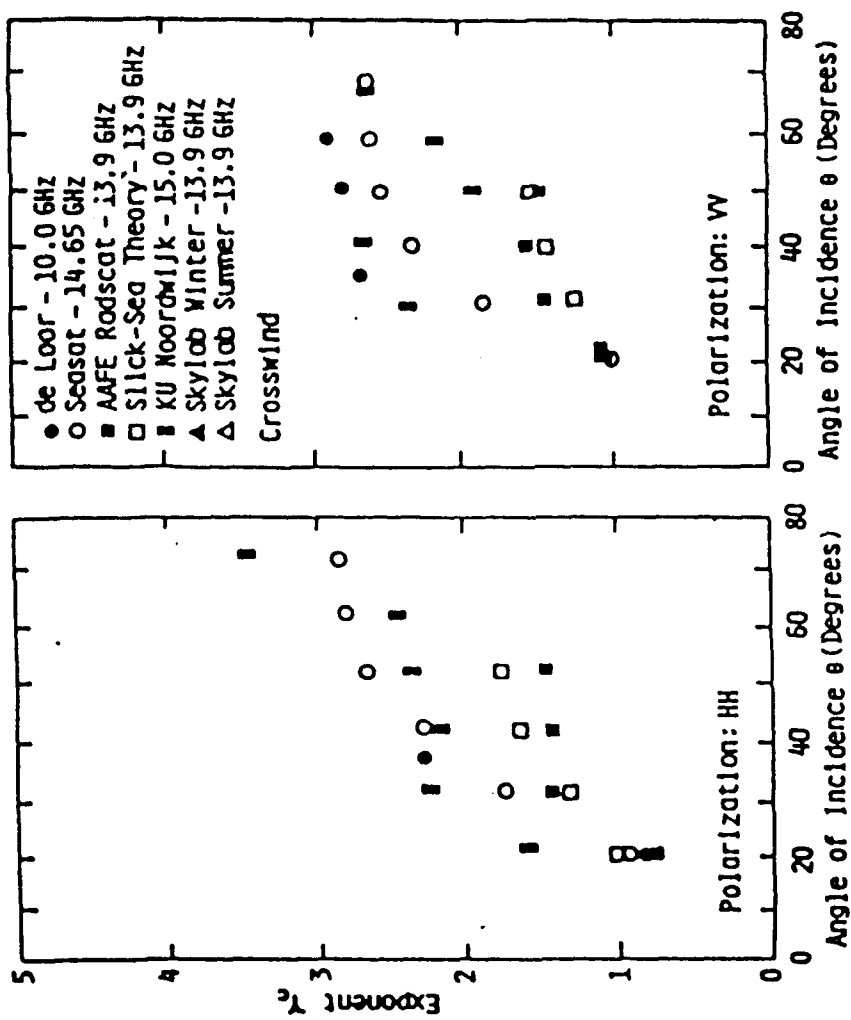


Figure 1-7 Crosswind speed response exponents from different experiments.

imaging of the ocean surface, and (3) developing a verifiable theory for SAR imaging of the ocean surface [18](Shemdin,O.H.,1988).

SAXON-CLT: A significant achievement from TOWARD is the determination that none of the then available theories on SAR imaging of long surface waves could explain all the SAR observations satisfactorily, particularly at higher frequencies like X band. To improve the theoretical models, the SAXON-CLT experiment was executed during September to October 1988 at the Chesapeake Light Tower (CLT), located 15 miles east of Virginia Beach, VA. The primary objectives were: (1) investigate the hydrodynamic modulation of short gravity and capillary waves by long surface waves and internal waves, (2) determine experimentally the modulations in radar waves, (3) test SAR imaging theories at X-Band and higher frequencies, and (4) investigate the influence of the microlayer on both active and passive remote sensing techniques [19](Popstefanja and McIntosh, 1989).

The SAXON-FPN experiment was conducted in November of 1990 with similar objectives.

#### 1-2. Background of SAXON experiment

The Synthetic Aperture X-Band Ocean Nonlinear Experiment (SAXON) was by American and German experimenters in the North Sea on and near the German Forschungsplattform Nordsee (FPN) in November of 1990. The primary objective of the experiment was to investigate the influence of the nonlinear parameters of the sea surface on the radar backscatter and the SAR

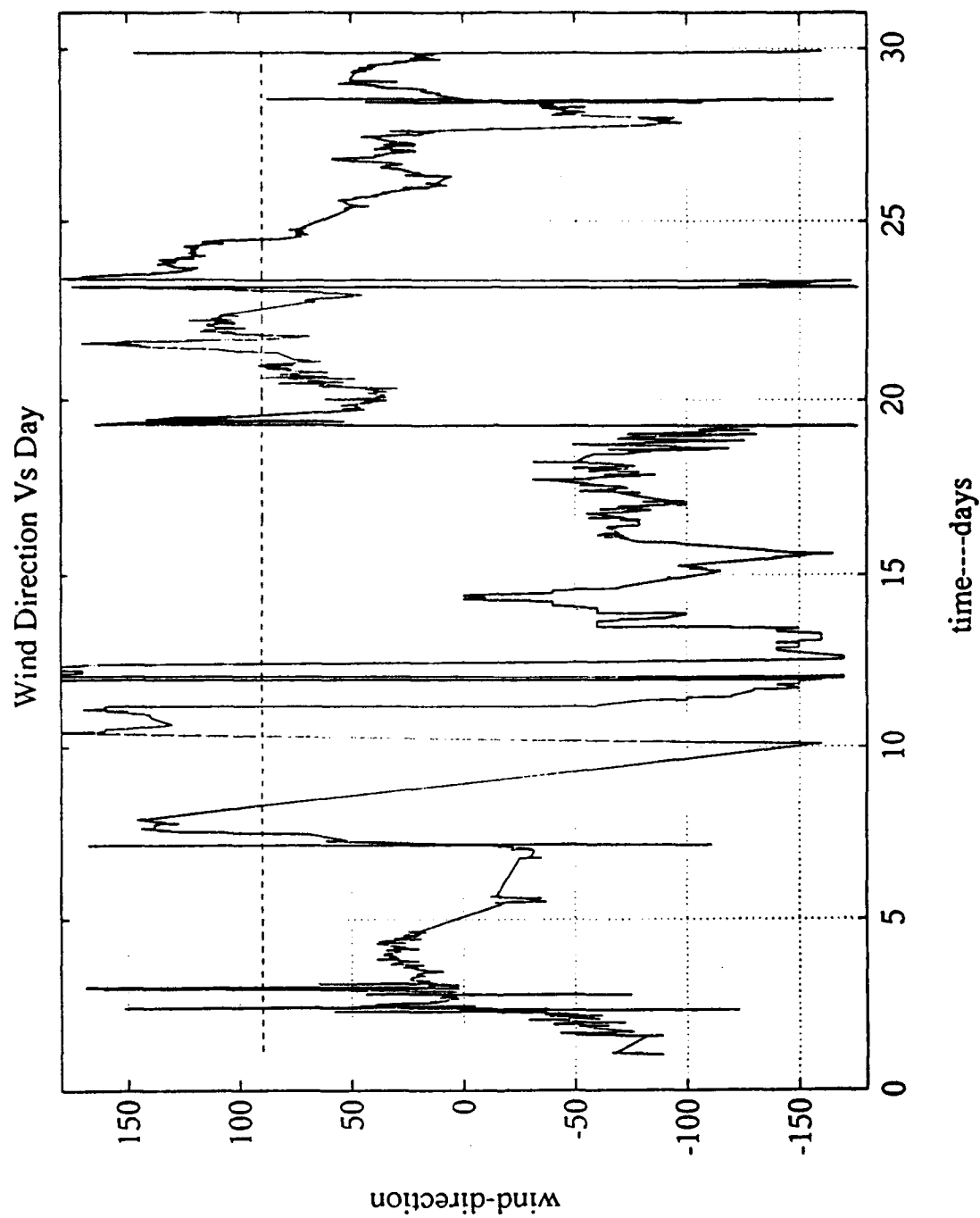


Figure 1-8 (b) The range of wind direction in SAXON-FPN during November, 1990.

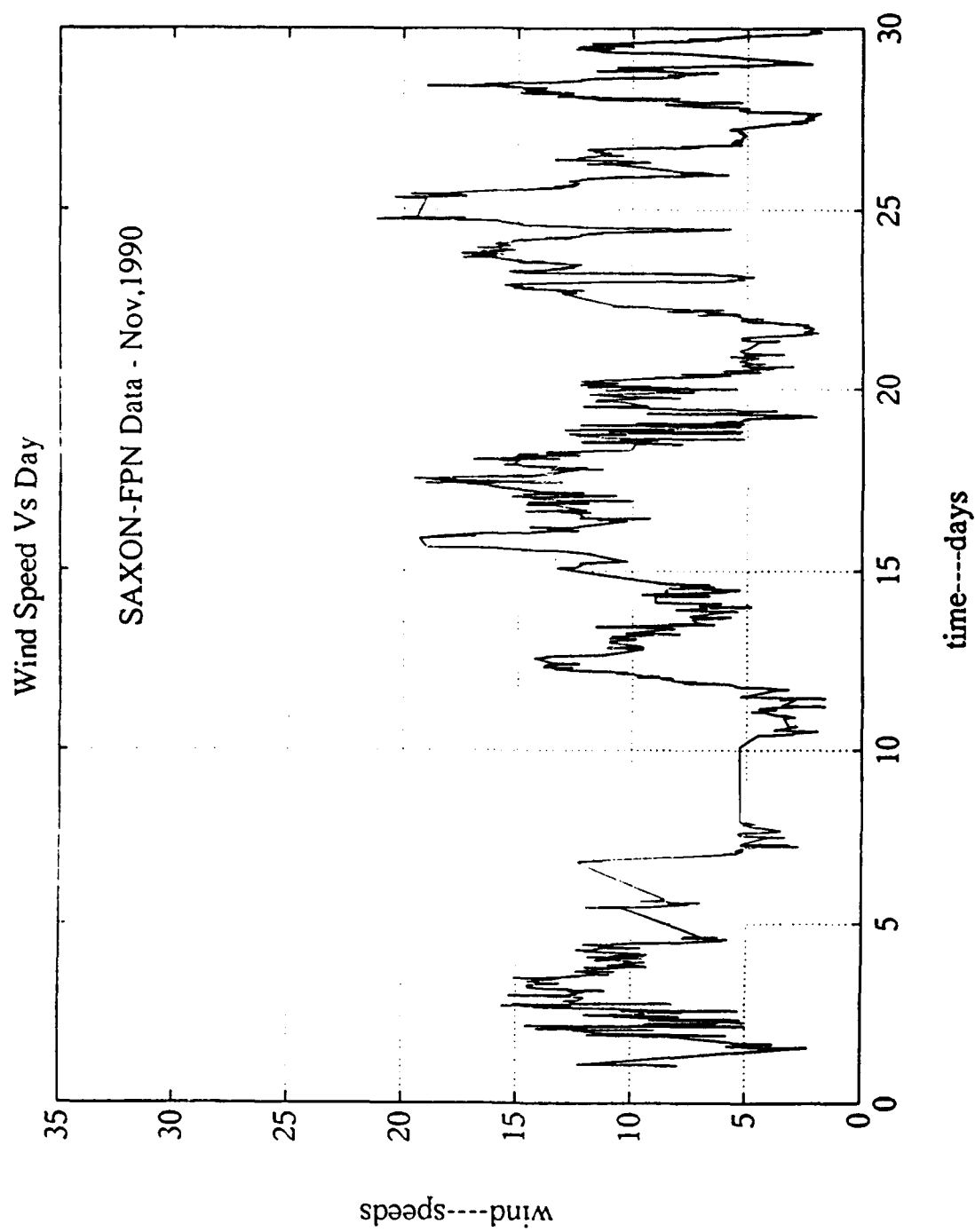


Figure 1-8 (a) The range of windspeed in SAXON-FPN



imagery at a variety of microwave frequencies under high sea-state conditions.

The Radar Systems and Remote Sensing Laboratory (RSL) of the University of Kansas joined this experiment by using a switched-beam vector-slope gauge/scatterometer(VSG) (Ka-band) and a dual-frequency X- and C-band FM-CW radar. One objective was to improve knowledge of the ocean -surface wind exponent  $\gamma$ , which is given by the empirical model,

$$\sigma^0 = A u^\gamma \quad (2)$$

where  $\sigma^0$  is the radar scattering cross-section,  $u$  is the ocean surface windspeed and  $A$  is a constant. Figure 1-8 (a) and (b) show the range of wind conditions encountered during the month.

In Chapter 2 of this report, the principles of windspeed exponent measurement are reviewed. Because of significant errors in windspeed measurement, and possibly in radar measurement, care in using regression is necessary. Two algorithms, orthogonal regression and ordinary linear regression, are studied. The measurements errors are also presented.

In Chapter 3, as an example of the windspeed exponent at 35 GHz, the SAXON experiments are studied in more detail. In this chapter, power measurement and data classification are discussed and the results from orthogonal regression and ordinary linear regression are compared.

Chapter 4 discusses variation of wind exponent with angle of incidence in detail. Bilinear regression is derived and used to explain the data. Finally, Chapter 5 states the conclusions.

## CHAPTER TWO

### WINDSPEED EXPONENT MEASUREMENT

The data from many aircraft scatterometer and spaceborne scatterometer experiments demonstrated that the radar backscattering coefficient  $\sigma^0$  over the ocean can be used to infer near-surface oceanic winds through a geophysical model function. In our case, we use the commonly accepted empirical model given by

$$\sigma^0 = Au^\gamma \quad (3)$$

Equation (2) can be expressed in log arithmetic form by

$$\log \sigma^0 = \log A + \gamma \log u \quad (4)$$

One can see that for this model,  $\log \sigma^0$  is a linear function of  $\log u$ . Therefore, to determine the coefficient  $\gamma$ , the slope of the linear equation (3), is the most important.

#### 2-1. Linear Regression Methods

We are concerned with the analysis of the relationship between two variables,  $x$  and  $y$ , where one variable ( $y$ ) is statistically dependent on the other ( $x$ ). Both variables are measured on a fixed scale, and the relationship between them is assumed to be linear. A method to fit a first-degree

polynomial function ( the linear function  $Y = b X + b_1$  is considered here ) to a set of observed paired scores is required. In our case, the Y variable is  $\sigma^0$  in dB and the X variable is log of ocean wind speed  $u$  , incidence angle or some other geophysical quantity.

Most experimenters use ordinary linear regression (OLR) of the radar scattering cross-section  $\sigma^0$  vs ocean surface windspeed  $u$ . The critical assumption of the OLR method is that we measure  $u$  without errors; that is, the measurement of the windspeed  $u$  is a true windspeed. Obviously  $u$  is not perfectly known without errors, so OLR gives a value of windspeed exponent  $\gamma$  that is not statistically correct. If one were to regress  $u$  vs  $\sigma^0$  instead, the value of  $\gamma$  obtained would be larger than usually reported. Detailed discussion of OLR can be found in mathematical statistics books [20], [21], [22].

In contrast, University of Kansas researchers often use orthogonal regression (OR), rather than OLR. In orthogonal regression, the best-fit line is that for which the mean-square distance normal to the regression line is a minimum. The slope of the best fit line, which represent the wind speed exponent  $\gamma$ , lies between the low value characteristic of OLR for  $\sigma^0$  vs  $u$  and the high value of OLR for  $u$  vs  $\sigma^0$ . With weighting to equalize the standard deviations, the scale factor  $f$  is simply the ratio of the standard deviations in the two directions, and it is also the geometric mean of the slopes obtained by regression  $\sigma^0$  vs  $u$ , and  $u$  vs  $\sigma^0$ . Thus the orthogonal regression line with slope  $b$  ( $\gamma$ ) must always lie between the other two regression lines. [23](R.K.Moore,1992).

The orthogonal-regression expression for the slope  $b$  of the regression line can be shown to be:

$$b = \frac{\sigma_y^2 - \sigma_x^2 \pm \sqrt{(\sigma_y^2 - \sigma_x^2)^2 + 4\sigma_{xy}^2}}{2\sigma_{xy}} \quad (5)$$

Here

$$\sigma_y^2 = E(y_i - m_1)^2, \quad \sigma_x^2 = E(x_i - m_2)^2, \quad \sigma_{xy} = E(y_i - m_1)(x_i - m_2) \quad (6)$$

where,  $x_i$  and  $y_i$  denote a sample point, and  $E(*)$  is the expectation operator,

The sample means are

$$m_1 = E(y), \quad m_2 = E(x) \quad (7)$$

[24](Cramer, 1946)

In the OR method, the assumption is that the  $\sigma^2$  and  $\log u$  have comparable scales.

An approximate  $1-\tau$  confidence interval for any given quantity  $c$  is

$$b_{21} - \frac{t_{N-2, \tau/2} s_2 \sqrt{1-\tau^2}}{s_1 \sqrt{N-2}} \leq c \leq b_{21} + \frac{t_{N-2, \tau/2} s_2 \sqrt{1-\tau^2}}{s_1 \sqrt{N-2}}$$

$t_{N-2, \tau/2}$  refers to the point with probability  $\tau/2$  to the right of the Student's distribution function with  $N-2$  degrees of freedom. [22] (Cramer, 1964).

For a two-dimensional distribution, we write

$$\bar{x} = \frac{\sum_1^N x_i}{N}, \quad \bar{y} = \frac{\sum_1^N y_i}{N}$$

and,

$$b_{21} = \frac{m_{11}}{m_{20}}; \quad s_1^2 = m_{20} = \sum_1^N \frac{(x_i - \bar{x})^2}{N}; \quad s_2^2 = m_{02} = \sum_1^N \frac{(y_i - \bar{y})^2}{N};$$

$$\tau s_1 s_2 = m_{11} = \sum_1^N \frac{(x_i - \bar{x})(y_i - \bar{y})}{N}$$

In particular, the quantity  $\tau$  defined by the relation

$$\tau = \frac{m_{11}}{s_1 s_2} \tag{12}$$

is the correlation coefficient of the sample.

In [25](Boggs, P.T. ,1990),[24], [23] and [22], OR is discussed in more detail.

Another approach to obtaining the best slope for a regression line is due to Wald[26](Wald,A. 1940). Here one divides the X axis (log u in our case) into two regions. One obtains mean values of the data for X and Y( $\sigma^2$  dB in our case) directions in each region. Then one joins the means with a straight line. Assuming the total number of sample points N is even, the estimator in its simplest form is

$$b = \frac{\sum_{i=1}^{N/2} y_i - \sum_{i=N/2+1}^N y_i}{\sum_{i=1}^{N/2} x_i - \sum_{i=N/2+1}^N x_i} \quad (13)$$

[26](Wald, A., 1940)

To compare the above methods, we find:

\* If there are only measurement errors in one (Y) of the variables, the ordinary least-square

estimation, OLR, produces the best results.

- \* The OR provides the best estimate when  $x$  and  $y$  have similar scales.

- \* For many cases where measurement error occur in both  $X$  and  $Y$ , the Wald method gives better results than either OLR or OR.

## 2-2. Measurement Errors

Errors occur in both radar and windspeed measurements. Radar errors may be due to noise, calibration problems, and errors in measuring the pointing angle. Windspeed errors may result from several different causes.

The wind that affects the surface ripple structure, and therefore the radar signal, is at the air-sea boundary. However, wind is usually measured with anemometers placed some distance above the surface. Standard heights for ships, for example, are 10 m and 19 m. When the atmosphere is turbulent, these measured winds are similar to those at the surface. For stratified atmospheres, however, the surface winds can be much less than at anemometer height. Some investigators use model functions to convert the anemometer measurements to friction velocity  $u^*$ . Other investigators convert measured winds at any height to equivalent winds at 10 m in a neutral atmosphere. These models depend on knowledge of the degree of stratification, usually obtained from air-sea temperature differences. They are far from perfect. See Figure.2-1. [27](R.A. Vaughan,1988).

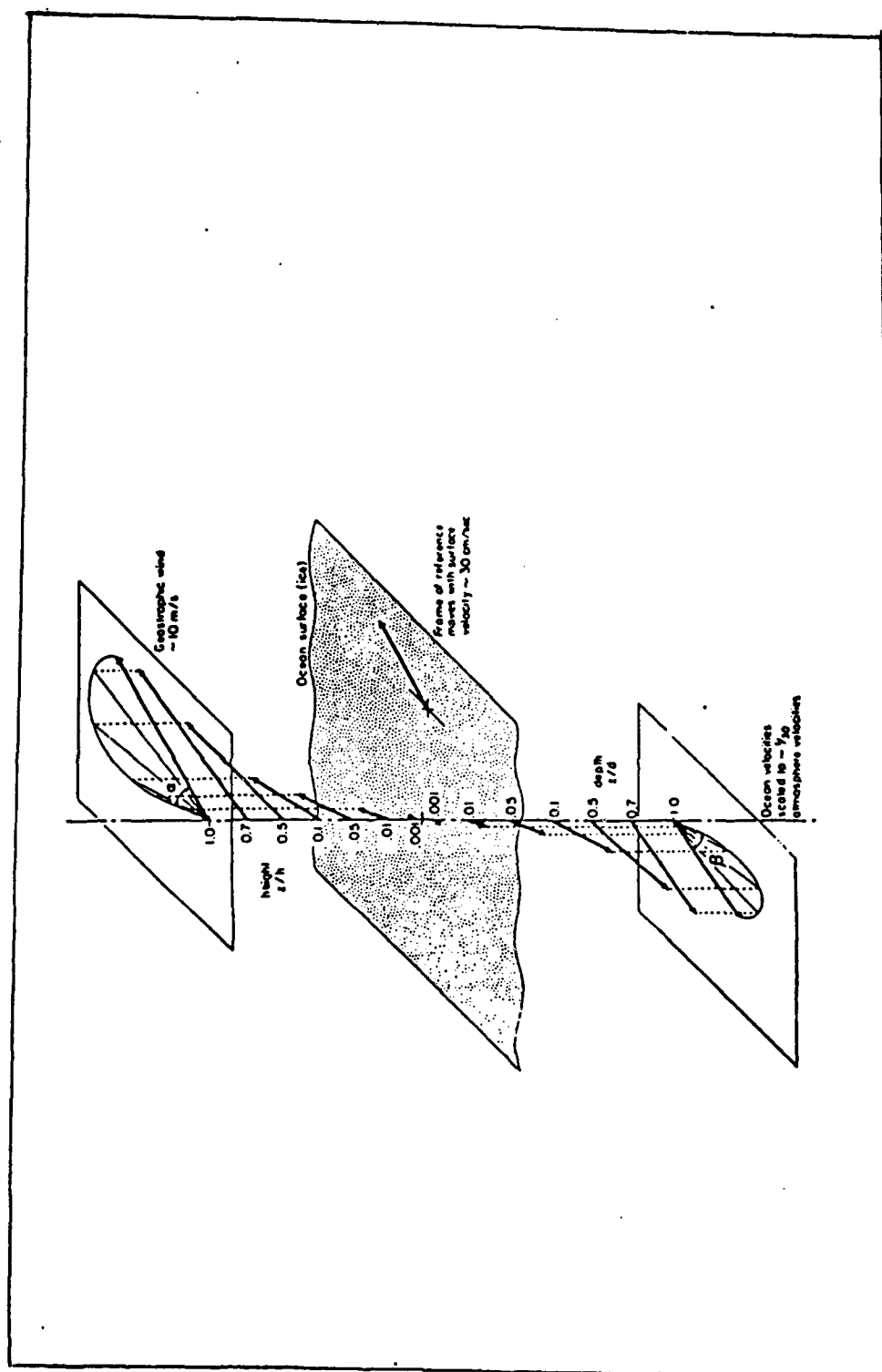


Figure 2-1 Linked hodographs of velocity vectors in oceanic and atmospheric PBLs.



The radar experimental results are given in terms of either (1) measured winds at anemometer height, (2) equivalent 10-m neutral-stability-atmosphere winds, or (3)  $u^*$  obtained by model functions. For this reason, one expects that the values obtained for both  $A$  and  $\gamma$ , which are magnitude coefficient and wind speed exponent, in

$$\sigma^0 = A u^\gamma$$

vary considerably between reports of different experiments.

Also, aircraft cannot measure directly at the anemometer location. Clearly, they must measure  $\sigma^0$  over some region that may extend several km from the anemometer. The winds at the aircraft measurement sites will be different, therefore, from those at the anemometer because of small-scale variations in the wind field.

For all of those reasons, one expects that most measurements of  $\sigma^0$  are less noisy than the wind measurements. However, most investigators still use the form of OLR that assumes perfect wind measurements, to calculate the wind exponent  $\gamma$ . Of course, more meaningful results would occur with OLR if the  $\sigma^0$  were chosen as the independent value. This would be true both because the relative error in  $\sigma^0$  may be less and because one wishes to use  $\sigma^0$  to estimate  $u$ , not  $u$  to estimate  $\sigma^0$ .

## CHAPTER THREE

---

### WINDSPEED EXPONENT MEASUREMENT IN SAXON-FPN

SAXON-FPN was conducted at the German Forschungsplattform Nordsee in November, 1990. The high sea state of the North Sea during November provides excellent conditions for investigations. Researchers of the University of Kansas used the 35-GHz (Ka-band) radar Vector Slope Gauge (VSG) and a dual-frequency FM-CW scatterometer radar, operating at C and X bands, to make instantaneous measurements of the two orthogonal components of the slope vector (along and perpendicular to the radar look direction). Unfortunately, the radar tracker of the dual-frequency scatterometer did not function properly under most conditions. Hence, most of the data collected with the X- and C-band radar could not be used for further analysis. Also, since an amplifier failed in the VSG, the data collected after November 27 are less useful for our research because of low signal-to-noise ratio. For these reasons, only Ka-band data (VSG) before November 27 are discussed here.

#### 3-1. Backscattering Power Measurement

During the SAXON-FPN experiment, KU's systems were installed on the northwestern corner of the platform at about 22 m altitude. See Fig. 3-1. The VSG used switchable antenna beams that illuminated three closely spaced footprints. The three beams were formed by a single parabolic reflector antenna with switched feeds. The antenna's 3-dB beam width was roughly

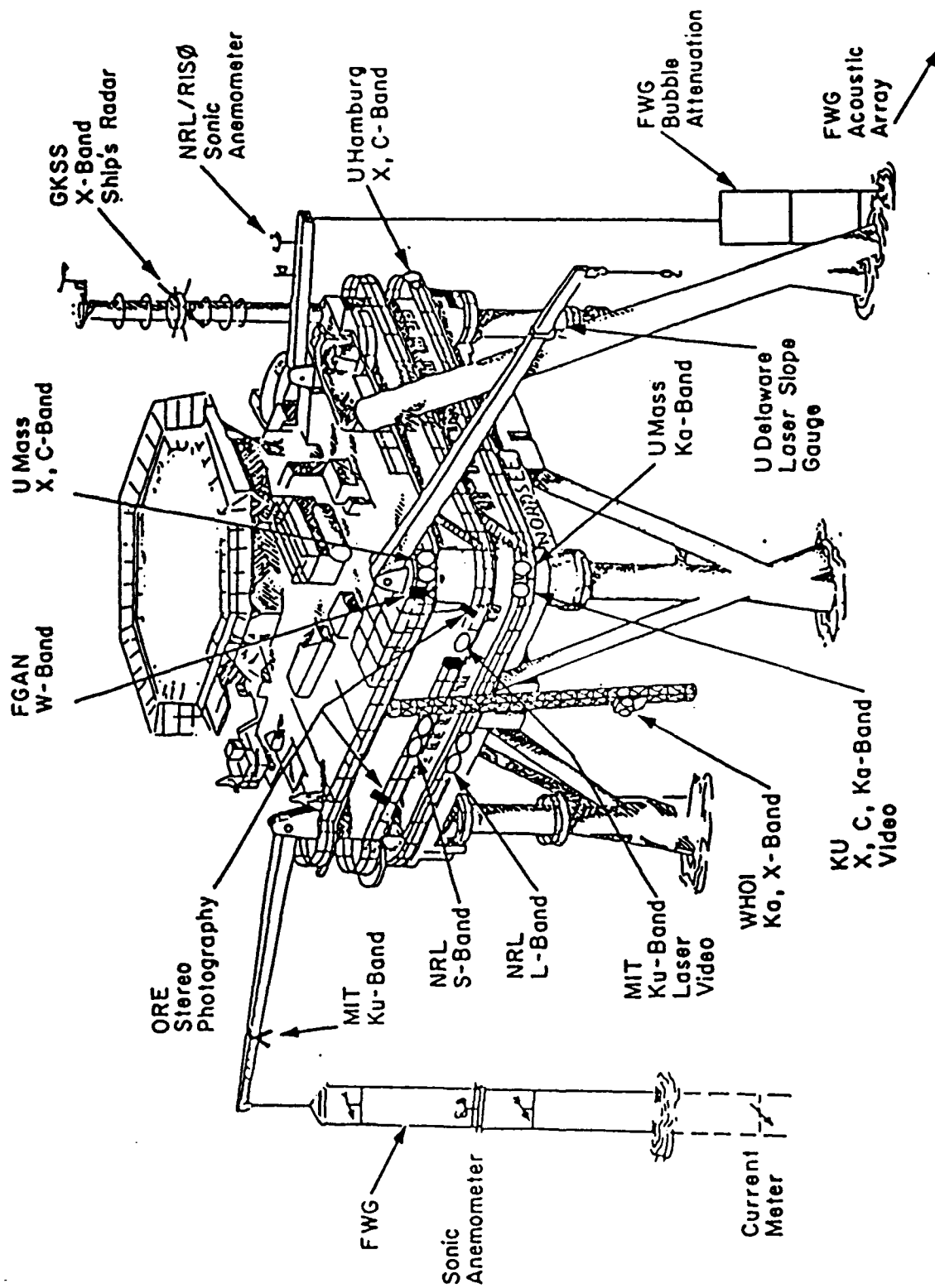


Figure 3-1(a) Diagram of Forschungplattform Nordsee.

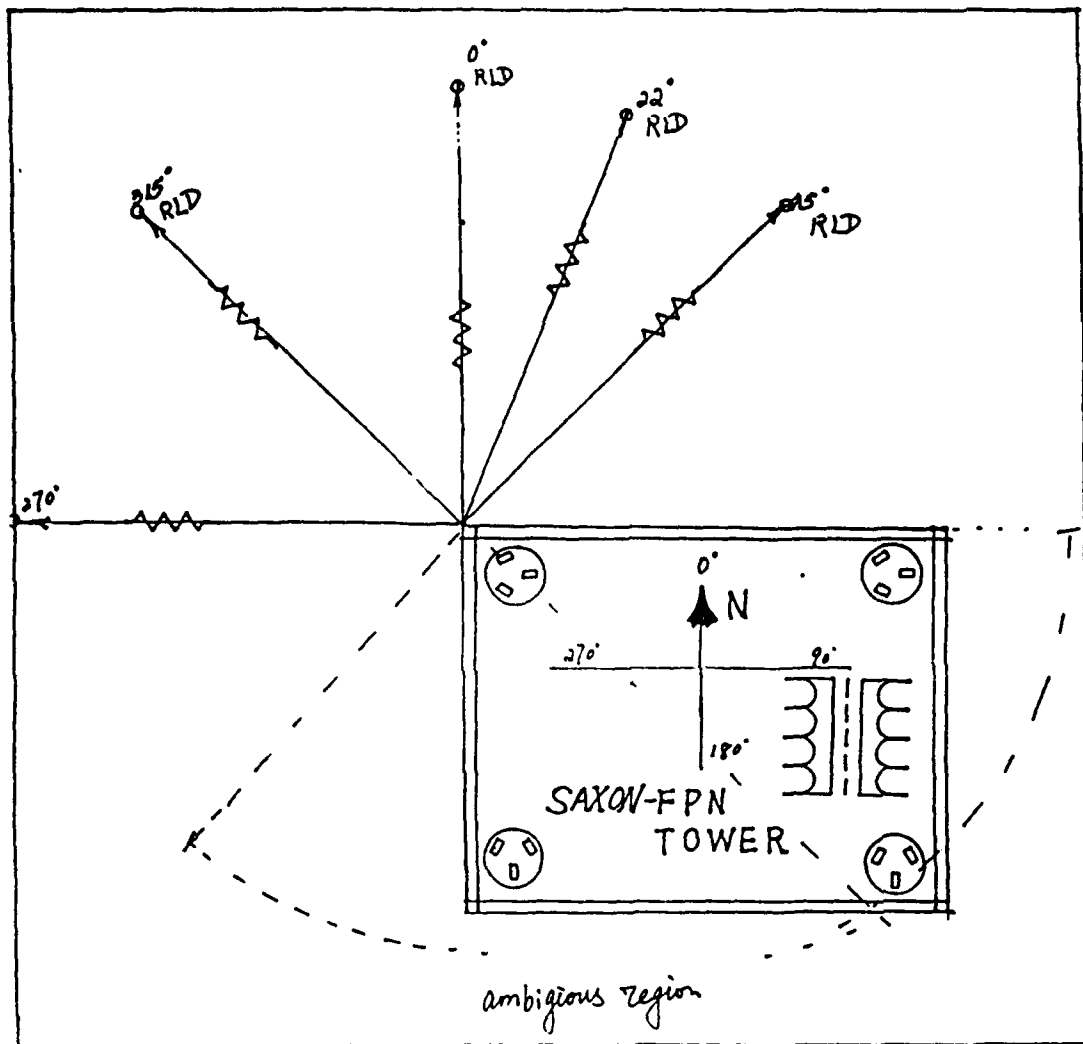


Figure 3-1 (b) Radar look direction and ambiguous region.

2°, and the beam-switching frequency was 30 Hz. Fig. 3-2 shows the footprint of the VSG. At each switching instant, one measurement of the range, and consequently the ocean wave-height, was obtained. The instantaneous wave height at the center of the three-beam footprint was obtained by averaging the height measurements from all three beams. The instantaneous backscattered power was detected by a mean-square detector for each beam. For more information, see [28](Bita B.Sistani, 1993).

Since every run of the radar observation was 50 minutes, over 30,000 data were obtained. Thus, in each 10-minute interval, the mean power estimate used about 6,000 data. Because the beams were not identical, normalization to beam 2 requires multiplying the first and the 3rd beams by 1.79 and 1.19. The normalized powers in each of the three beams during 10 minutes were averaged. After that, the three averaged-power values were averaged again to obtain the mean power of all the three beams in the 10 minutes. Some of these data are shown in the Table 1 and Table 2.

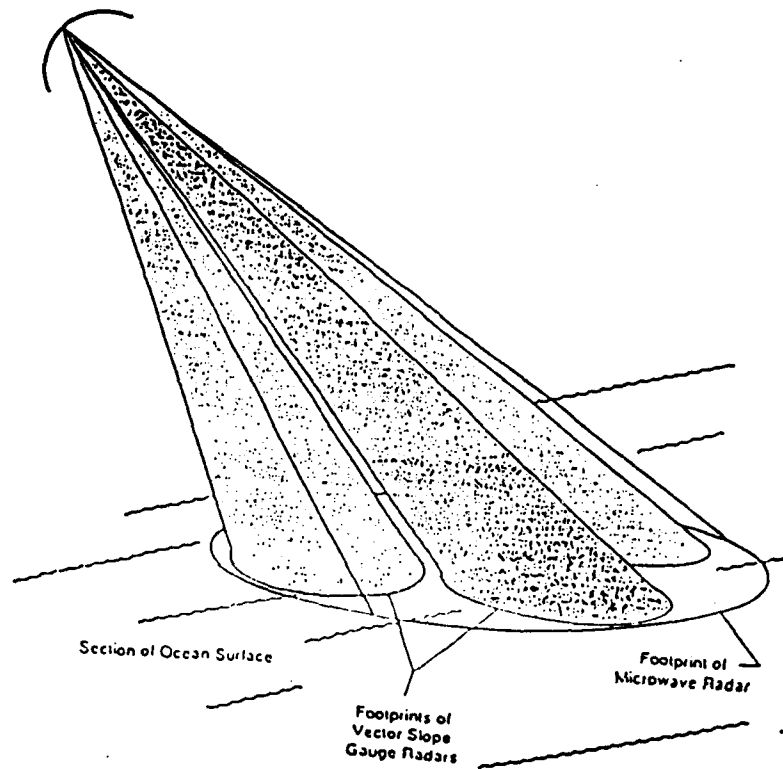


Figure 3-2 Configuration of the Vector Slope Gauge system

**Table I**

Part of SAXON Upwind data

RUN No.	MEAN- POWER	WIND- SPEED	WIND- DIR	RLD-DEG	WAVE- DIR	INC-ANG DEG
11191047	1.507	9.04	315	315	282	47
	1.409	8.65	318	315	282	47
	1.404	8.32	314	315	282	47
	1.357	8.98	309	315	282	47
	1.506	8.25	311	315	282	47
11191205	1.231	7.27	302	315	282	47
	1.252	7.65	294	315	282	47
	1.077	9.41	289	315	282	47
	1.318	8.73	234	315	282	47
	1.536	8.73	283	315	286	47
11191749	1.208	9.24	272	315	284	47
	1.558	7.78	273	315	286	47
	1.583	8.91	291	315	286	47
	1.339	8.05	301	315	286	47
	1.465	7.18	297	315	286	47

11191846	1.629	9.44	301	315	288	47
	0.977	6.27	302	315	288	47
	0.721	4.67	287	315	288	47
	0.584	4.11	283	315	288	47
	0.340	4.11	273	315	288	47
11192246	0.885	6.48	297	315	278	47
	0.638	4.99	300	315	278	47
	0.667	4.27	295	315	278	47
	0.467	4.27	287	315	278	47
	0.432	4.11	296	315	278	47
11211114	0.311	5.80	58	45	356	45
	0.208	5.33	61	45	356	45
	0.222	5.56	64	45	356	45
	0.159	5.56	69	45	351	45
	0.143	5.56	75	45	351	45
11211213	0.086	3.38	83	45	354	45
	0.094	2.58	71	45	354	45
	0.103	3.07	59	45	354	45
	0.107	3.54	58	45	354	45
	0.190	4.11	53	45	0	45



**Table II**

**PART OF SAXON CROSSWIND DATA**

RUN NO.	MEAN- POWER	WIND- SPEED	WIND- DIR	RLD-DEG	WAVE- DIR	INC-ANG DEG
11200925	0.117	3.95	55	315	279	47
	0.086	4.19	50	315	279	47
	0.084	4.19	48	315	279	47
	0.094	4.19	53	315	279	47
	0.086	3.95	64	315	279	47
11201733	0.14	7.73	48	315	305	45
	0.151	7.94	48	315	307	45
	0.157	7.37	46	315	307	45
	0.189	7.37	44	315	307	45
	0.169	7.37	46	315	307	45
11201839	0.194	7.43	54	315	307	45
	0.188	7.10	52	315	315	45
	0.193	6.85	49	315	315	45
	0.163	7.11	46	315	315	45
	0.144	6.62	46	315	315	45

11202305	0.134	5.68	46	315	59	45
	0.124	5.76	47	315	59	45
	0.114	5.68	41	315	53	45
	0.180	6.76	39	315	53	45
	0.133	6.27	38	315	53	45
11230953	0.480	8.52	110	22	128	45
	0.533	8.71	107	22	128	45
	0.608	8.65	110	22	128	45
	0.586	8.19	115	22	128	45
	0.536	8.98	120	22	128	45
11231107	0.450	7.35	124	22	128	45
	0.471	7.73	113	22	128	45
	0.396	7.45	111	22	128	45
	0.417	6.86	113	22	128	45
	0.408	7.00	113	22	128	45
11231243	0.232	7.00	96	22	119	45
	0.245	6.78	93	22	119	45
	0.194	6.72	93	22	119	45
	0.195	7.00	88	22	119	45
	0.203	7.00	90	22	119	45

### 3-2. Wind Data Classification

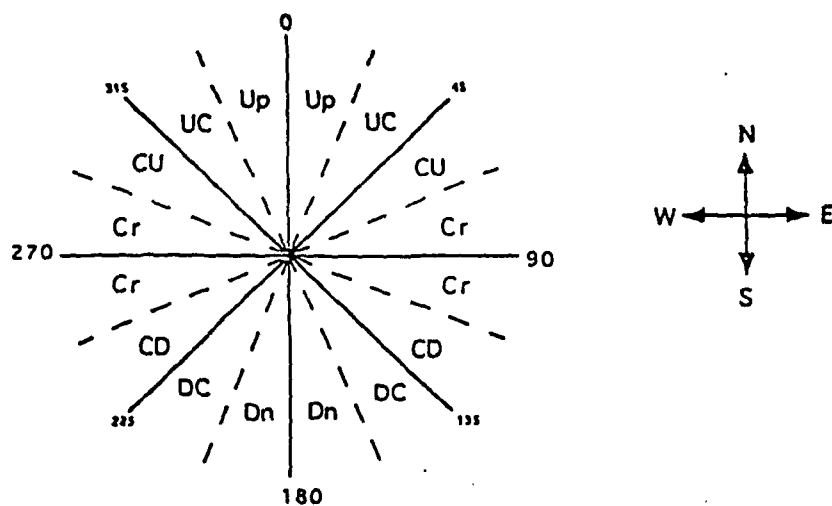
In microwave remote sensing, the ocean surface wind direction and speed as well as the wave direction are very important. Most of the author's research work in the past two years was to study the behavior of the radar scattering cross-section under different wave and wind conditions.

Fig 3-3 illustrates regions of different wind or wave classification with an explanation of what each abbreviation means. For example, when the radar look direction (RLD) has  $\pm 20^\circ$  difference from the wind or wave direction, the radar is defined to be looking Up wind or Up wave. To help understand the effect of wind and wave on radar cross-section  $\sigma^\circ$ , two cases for each of the following wind and wave categories are discussed next:

- (i) Upwind under both Up and Cross-wave or only Upwave
- (ii) Crosswind under both Up and Cross wave or only Upwave

Since downwind and downwave data are corrupted by the shadow of the tower, results from CD (Crosswind-Downwave), DC and Dn are not reported here. Also, for each case mentioned above, only sample results are presented. Figure 3-4 shows the range of wind conditions encountered from 19 to 23 November.

- (i) Case I: Upwind under both Up and Cross wave or only Upwave



Up = Up direction  
 UC = Up/Cross direction  
 CU = Cross/Up direction  
 Cr = Cross direction  
 CD = Cross/Down direction  
 DC = Down/Cross direction  
 Dn = Down direction

Figure 3-3 Regions of different wave or wind condition.

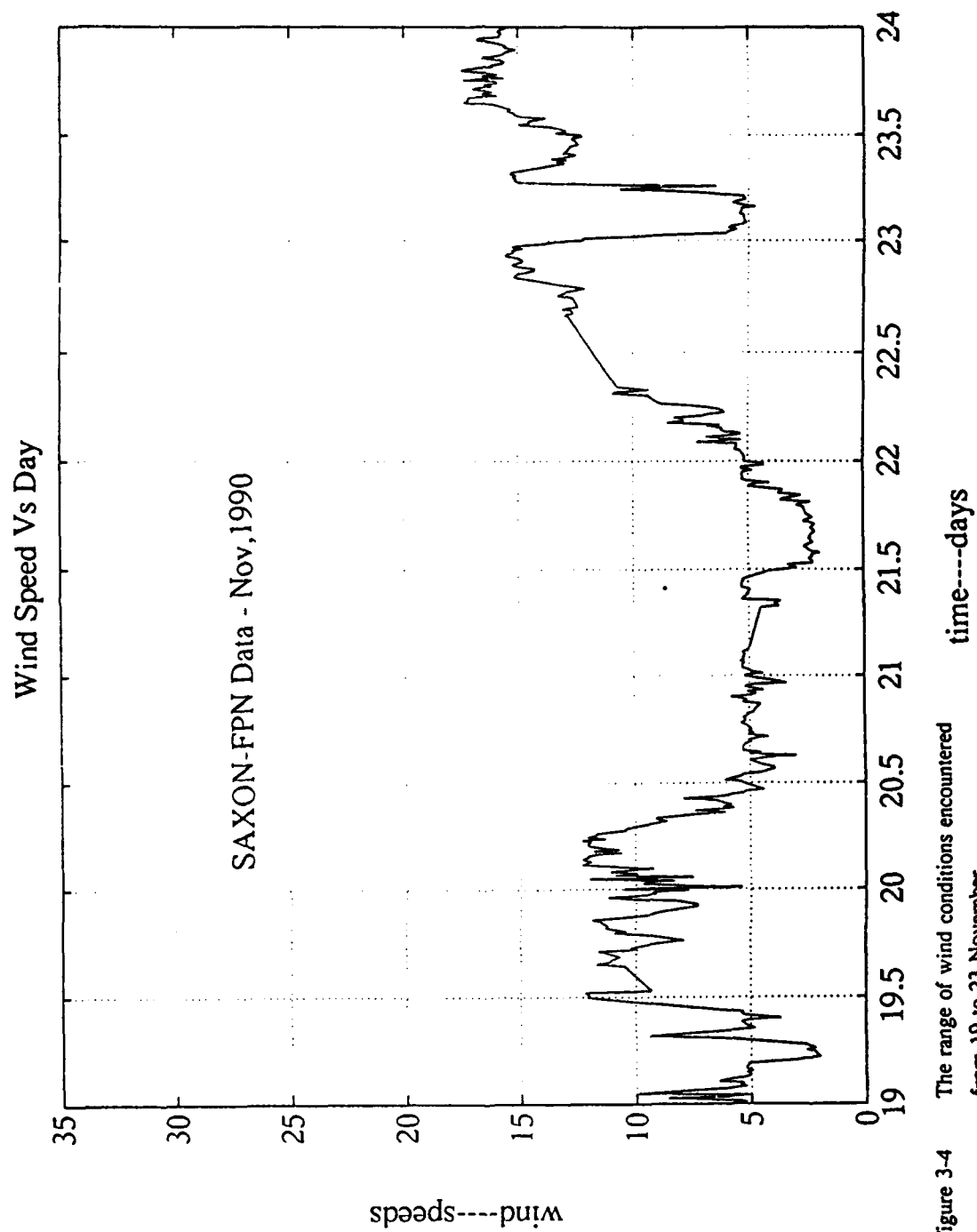


Figure 3-4 The range of wind conditions encountered from 19 to 23 November.  
(a) Wind speed vs day

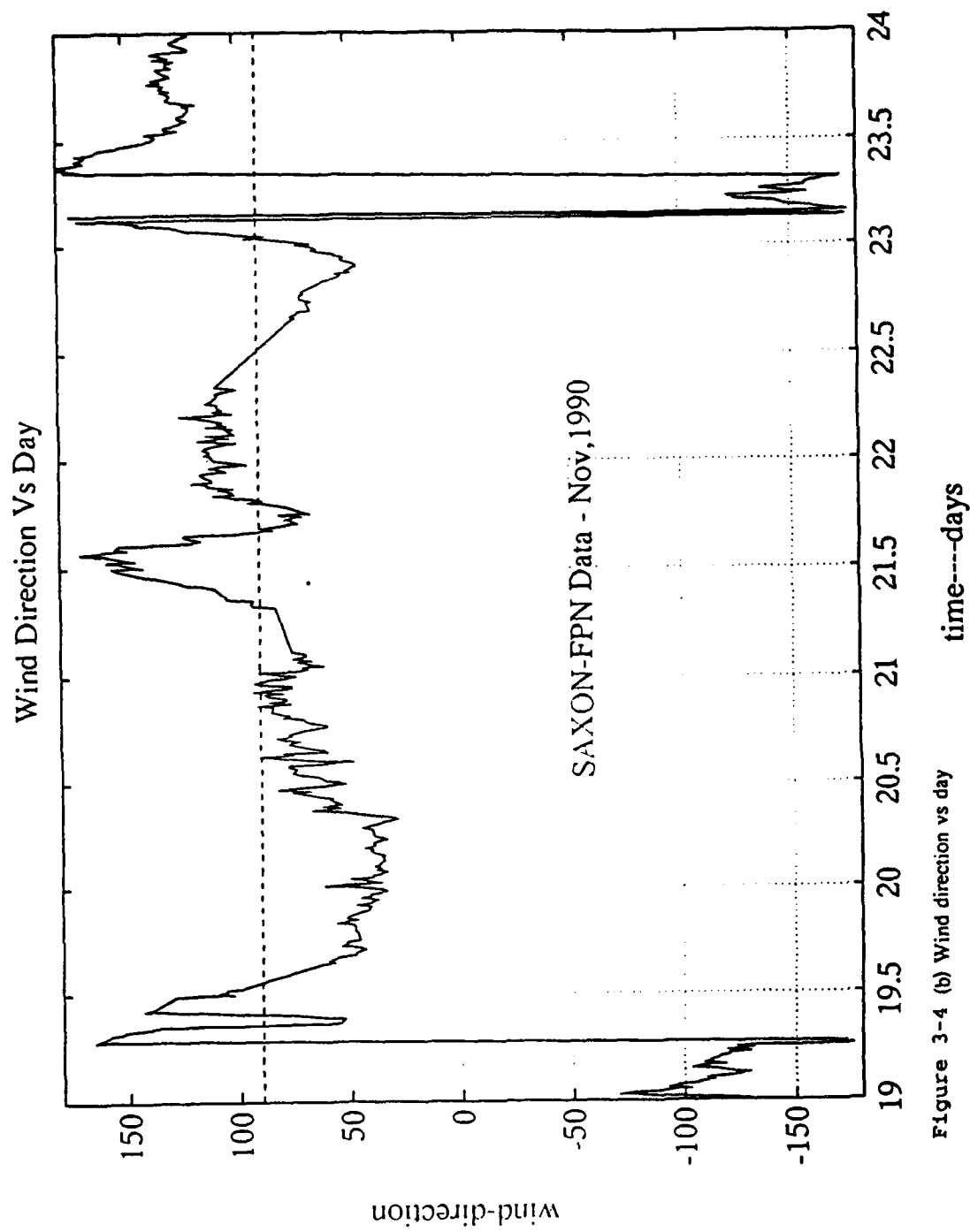


Figure 3-4 (b) Wind direction vs day

In this case two situations should be considered. (a) First we consider the effect on radar cross-section  $\sigma^0$  under both Up and Cr wave conditions. In this situation, the values of the wind exponent  $\gamma$  (slope of the linear equations) obtained by OLR, OR and  $\log u$  vs  $\sigma^0$  regression are higher than most previous investigators found at lower frequencies. Figure 3-5 shows the  $\gamma$  was 3.11 by OR, or 2.33 by OLR when wind speed varied from 3.5 to 10 m/s. The standard deviation is only 0.851.

(b) Now consider the results if the data with Crosswave are removed from above situation. Figure 3-6 shows that the value of  $\gamma$  obtained by OLR or OR are much lower than the data that include Crosswave. The slopes of the lines are 1.64 by OR and 1.54 by OLR while the standard deviation is 0.955. These slopes are close the value 1.6 to 2.0 which most of other investigators obtained.[4] (Moore, R.K. vol. iii,1986).

(ii) Case II: Crosswind under both Up and Crosswave or only Upwave

This category refers to the case when the surface wind is considered to be orthogonal to the RLD, while the long wave is either Up or Cross. That is, wind and wave directions are nearly orthogonal or close together. (a) If we do not remove the data with Cross wave from our calculation, we obtain the higher values of  $\gamma$  shown in Figure 3-7. The slopes of the lines are 2.04 by OLR and 3.26 by OR. The standard deviation is 0.769. (b) However, when only Up wave data is considered, the resulting lower  $\gamma$  and higher standard deviation are shown in Figure 3-8. The slopes are 1.004 by OLR and 1.161 by OLR and the standard deviation is 0.881.

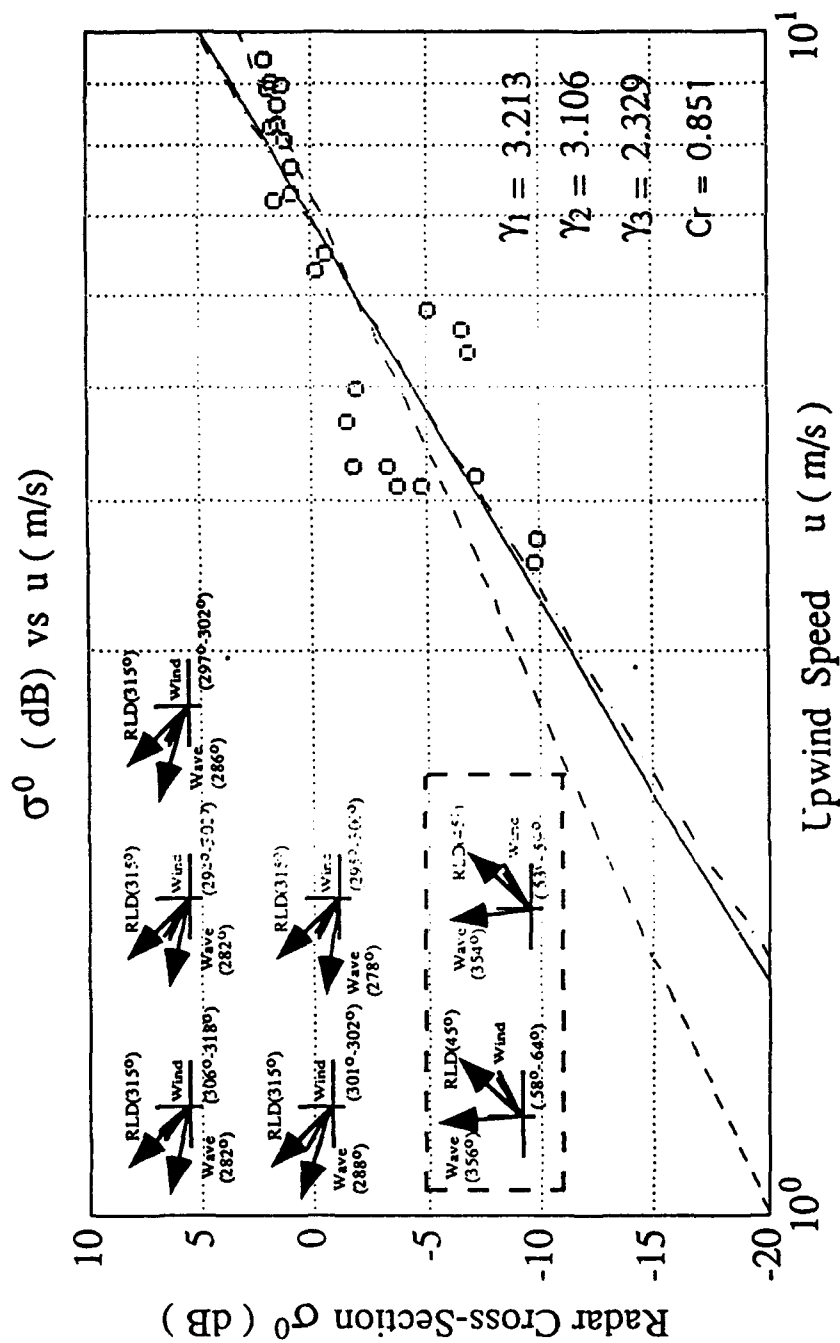


Figure 3-5 Case 1: (a) Upwind under both Up Cross-wave.



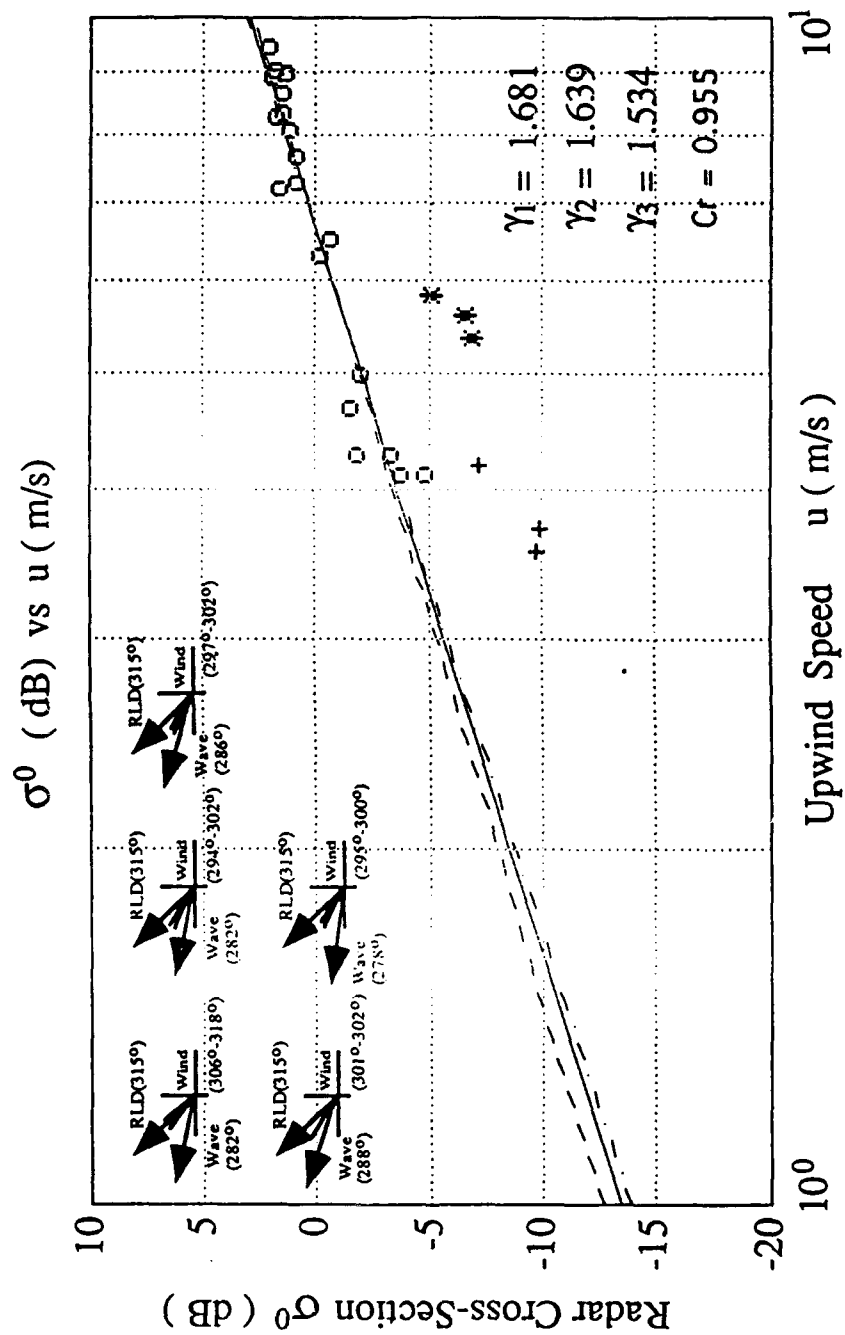


Figure 3-6 Case I: (b) Upwind under only Upwave.

### 3-3. Results

From above discussion, we find the following:

- i. Most measurements of  $\sigma^0$  are less noisy than the wind measurements. In spite of this, most investigators use OLR, which assumes perfect wind measurements. Thus, the results from OLR can be significantly in error for scattered measurement points.
- ii. The wave direction caused different wind exponents  $\gamma$  calculated by OR or OLR. Thus, one should consider both wind and wave directions in estimating radar backscatter or inverting to obtain the wind vector.
- iii. The wind exponents  $\gamma$  in Crosswind cases are higher than in the Upwind case.
- iv. The highest  $\gamma$  occurs for the Crosswind, Crosswave condition.
- v. The wind exponents  $\gamma$  independent wind speed but dependent wind direction.  
Cross-wind exponent > Downwind > Upwind.

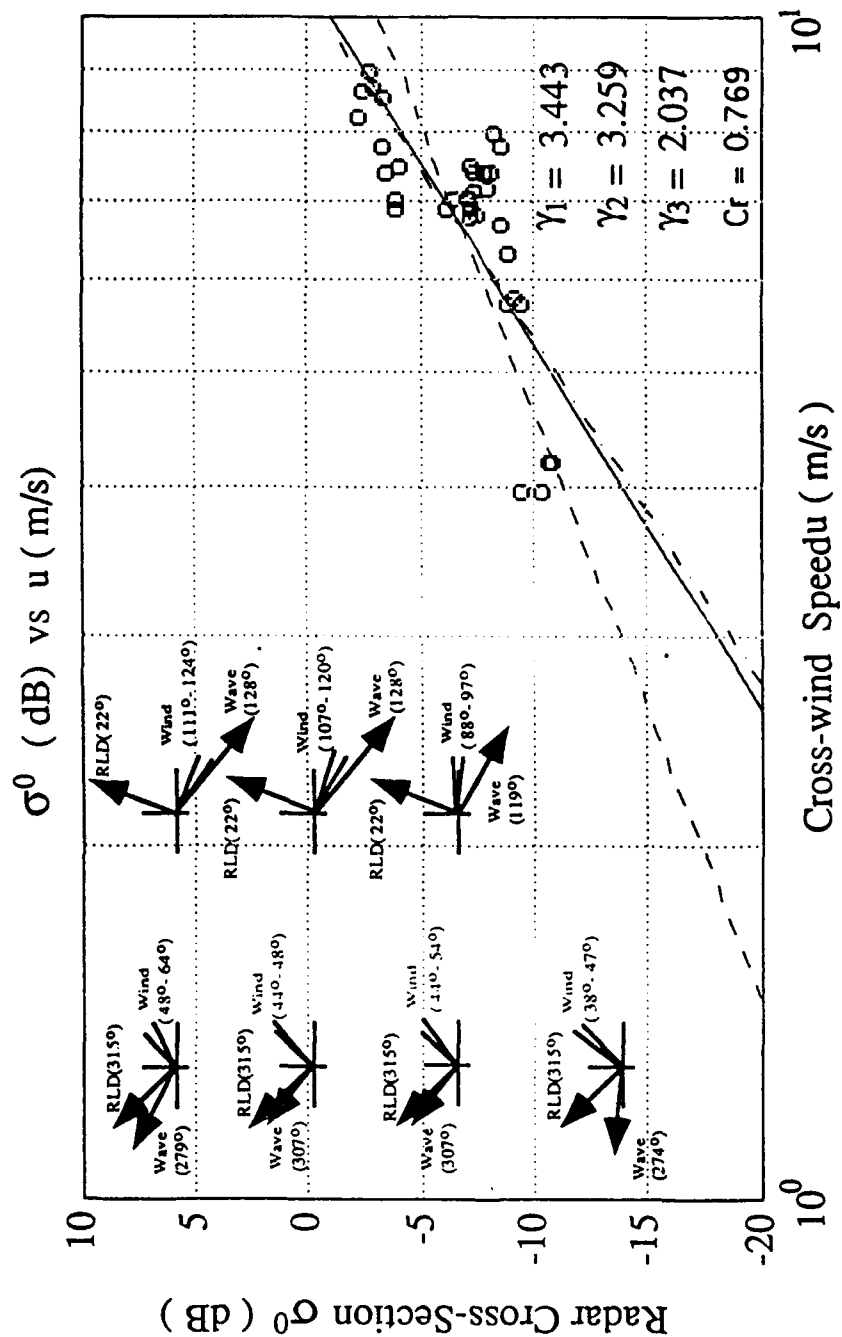
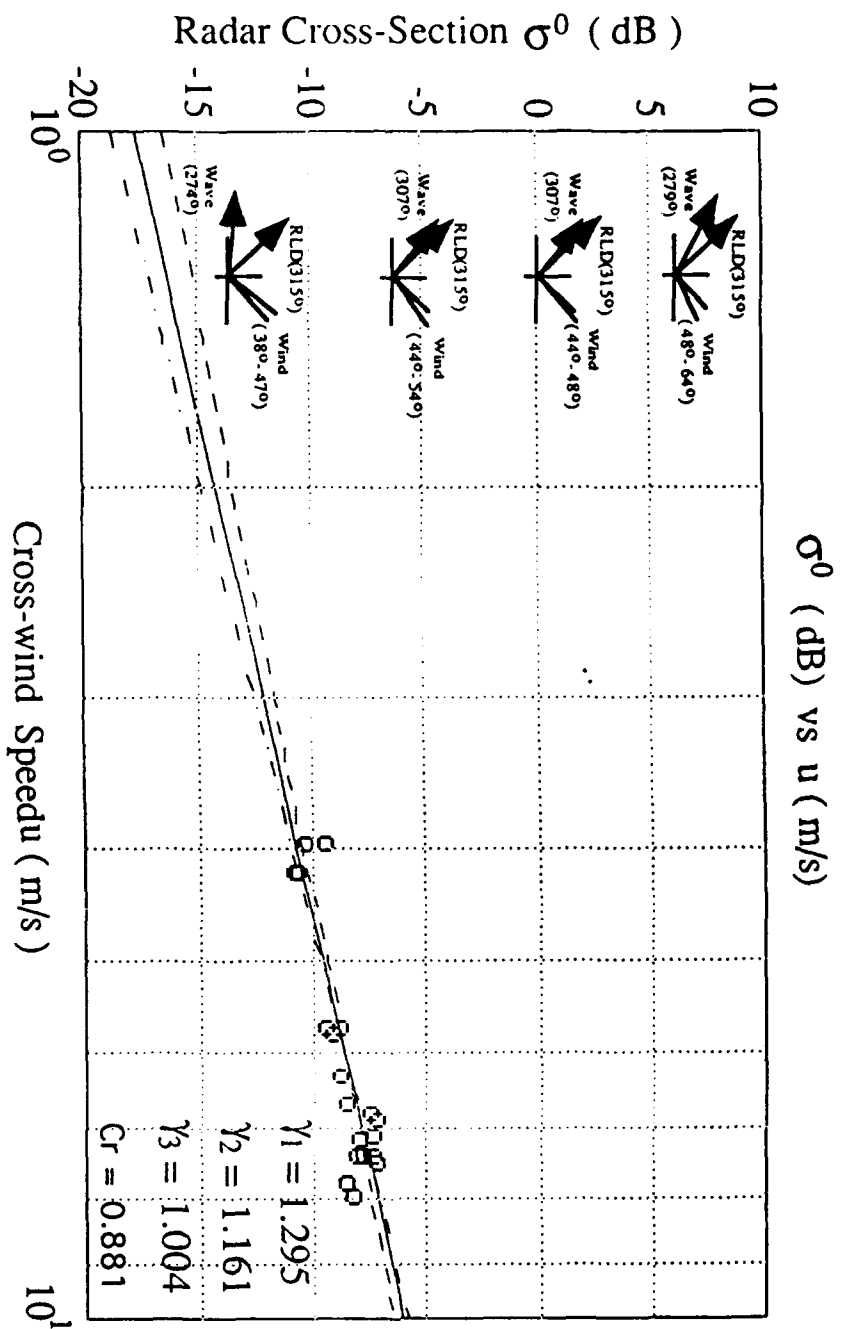


Figure 3-7 Case II: (a) Crosswind under both Up Cross-wave.



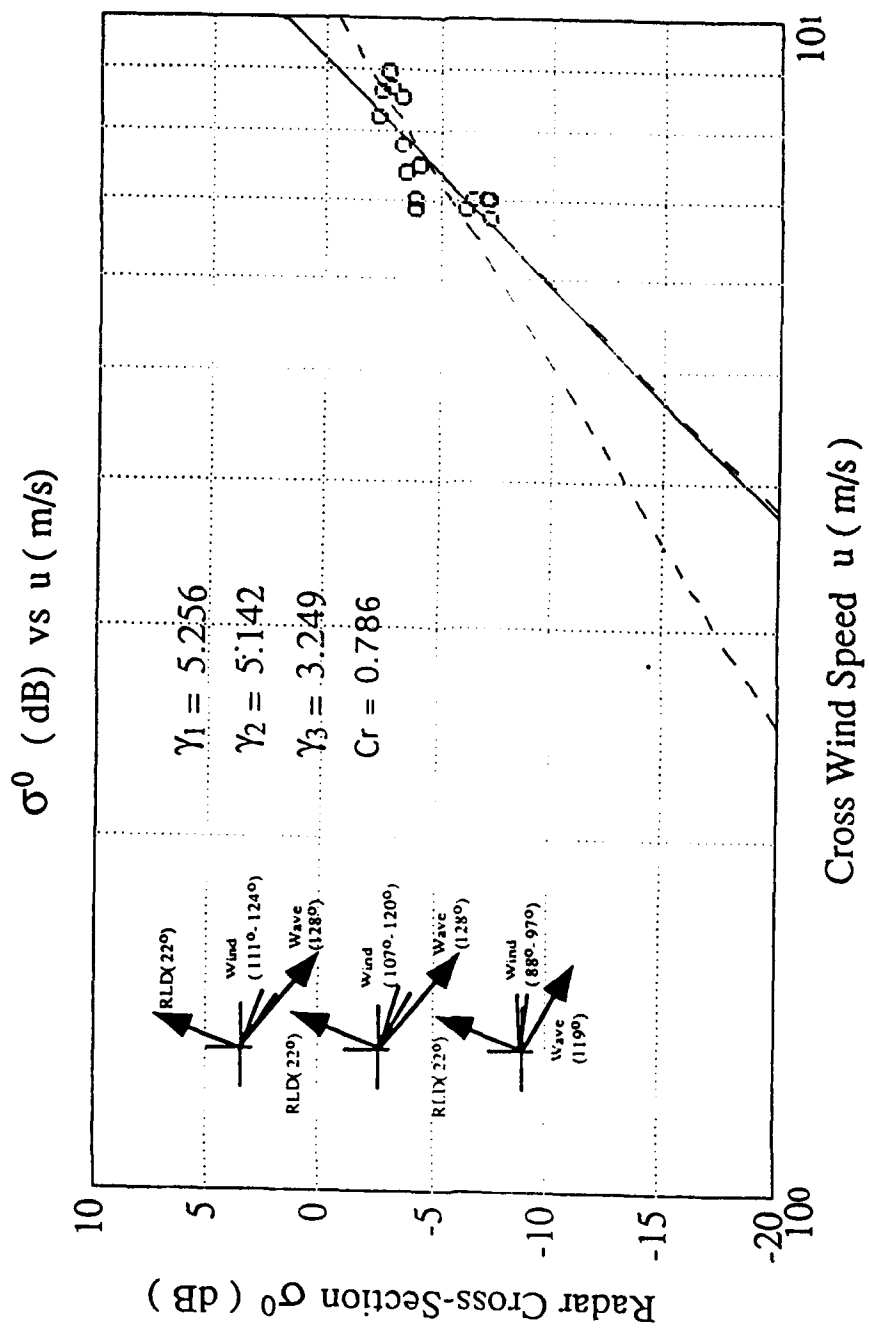


Figure 3-9 Case II: (c) Crosswind under only Cross wind

## CHAPTER FOUR

-----

### VARIATION OF WIND EXPONENT WITH ANGLE OF INCIDENCE

Experimental results are available at several frequencies and under a variety of conditions. In every case, the experimenters report their results in terms of growth of scattering coefficients proportional to windspeed raised to some exponent  $\gamma$ , with the exponent being different for different radar look directions relative to upwind. The results from different experiments give different values of  $\gamma$ , but combining them permits us to perform regression to get the best estimate possible from the data. Values of  $\gamma$  from several previous experiments are plotted in Figures 4.1, in which the reported values of the windspeed exponent vary quite widely. Note that the values from the KU Noordwijk experiment are higher than those from other experiments because OR gives higher values than the OLR used by other investigators.

#### 4-1. Derivation of Bilinear Regression

When one examines the data in the figures, one can reach the conclusion that the variation with angle of incidence falls into two regimes: below  $40^\circ$  and above  $40^\circ$ . Below  $40^\circ$  the exponent increases rapidly with incidence angle. Above  $40^\circ$  it increases more slowly. For this reason, we elected to use a bilinear regression technique to fit the angular variation of  $\gamma$ . Although there is no particular reason to expect the variation to be linear in either angular regime, the spread in the data is such that use of a nonlinear form is not justifiable.

Let us separate all measured  $\gamma$ s into two groups: the incidence angles are  $\leq 40^\circ$  in a group (A) and  $> 40^\circ$  in group (B). Suppose the total number of data is  $N$ , the number of groups for (A) is  $N_1$  and the number of groups for (B) is  $N_2$ . Also, let "x" represent the incidence angle and "y" the value of the wind exponent  $\gamma$ , we join the two linear regression equations at the point  $(X_0, Y_0)$ , where  $X_0=40^\circ$ . Therefore the two equations can be written as:

$$Y_i = Y_0 + (X_i - X_0) b_1, \quad (X_i \leq X_0) \quad (15)$$

and

$$Y_i = Y_0 + (X_i - X_0) b_2, \quad (X_i \geq X_0) \quad (16)$$

where,  $b_1, b_2$  are the slopes of the regression lines.

Now set,

$$S = \sum_{i=1}^N (Y_i - Y)^2 \quad (17)$$

If we want to get the minimum of S, we take the partial derivative with respect to S.

Letting,

$$\partial S / \partial Y_b = 0$$

the equation yields

$$\sum_1^N Y_i - Y_b N - b_1 \sum_1^{N_1} X_i - b_2 \sum_1^{N_2} X_i + b_1 X_b N_1 + b_2 X_b N_2 = 0 \quad (18)$$

Also setting the partial derivative of S with  $b_1$  equal to zero,

$$\partial S / \partial b_1 = 0$$

Then,



$$\sum_1^{N_1} Y_i X_i - Y_b \sum_1^{N_1} X_i - b_1 \sum_1^{N_1} X_i^2 + 2b_1 X_b \sum_1^{N_1} X_i - X_b \sum_1^{N_1} Y_i + X_b Y_b N_1 - b_1 X_b^2 N_1 = 0$$

(19)

Finally, let

$$\partial S / \partial b_2 = 0$$

Hence,

$$\sum_1^{N_2} Y_i X_i - Y_b \sum_1^{N_2} X_i - b_2 \sum_1^{N_2} X_i^2 + 2b_2 X_b \sum_1^{N_2} X_i - X_b \sum_1^{N_2} Y_i + X_b Y_b N_2 - b_2 X_b^2 N_2 = 0$$

(18)

Rearranging the equations, we get the following equation set,

$$Y_b N + b_1 \left( \sum_1^{N_1} X_i - X_b N_1 \right) + b_2 \left( \sum_1^{N_2} X_i - X_b N_2 \right) = \sum_1^N Y_i \quad (21)$$

$$Y_b \left( \sum_1^{N_1} X_i - X_b N_1 \right) + b_1 \left( \sum_1^{N_1} X_i^2 - 2X_b \sum_1^{N_1} X_i + N_1 X_b^2 \right) = \sum_1^{N_1} Y_i X_i - X_b \sum_1^{N_1} Y_i \quad (22)$$

and,

$$Y_b \left( \sum_1^{N_2} X_i - X_b N_2 \right) + b_2 \left( \sum_1^{N_2} X_i^2 - 2X_b \sum_1^{N_2} X_i + N_2 X_b^2 \right) = \sum_1^{N_2} Y_i X_i - X_b \sum_1^{N_2} Y_i \quad (23)$$

Solving the above equation set,  $Y_b$ ,  $b_1$  and  $b_2$  can be obtained.

Using the data of Seasat, KU Noordwijk, Skylab, etc. experiments, the relationships with the incidence angles for upwind, and downwind in Ku band for VV polarization show in Figure 4-1 and Figure 4-2, while Figure 4-3 and Figure 4-4 show the relationships for HH polarization. All the slopes and the standard deviations for each curve region are summarized in Table 3

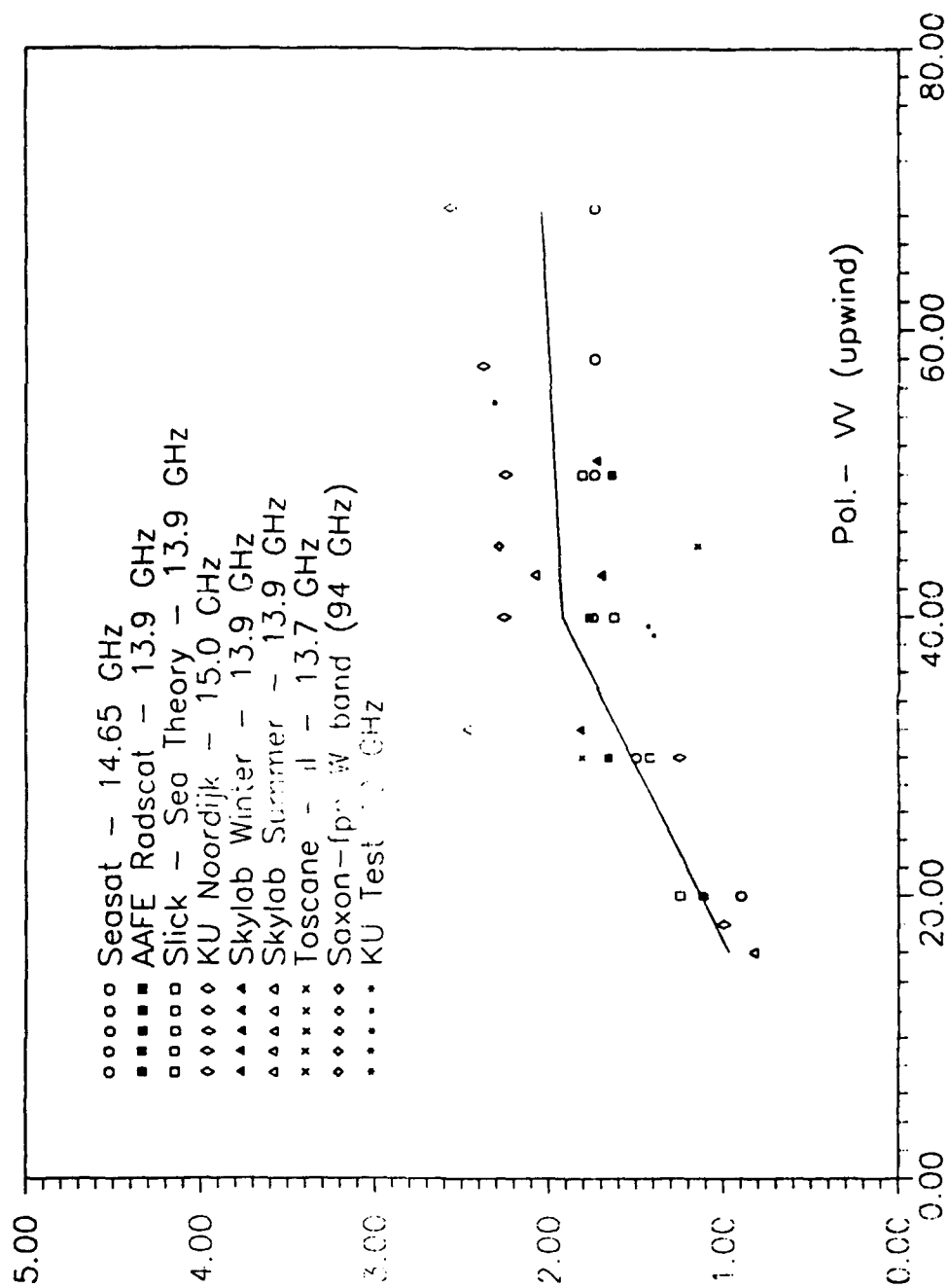


Figure 4-1 Bilinear regression for Upwind under VV polarization.

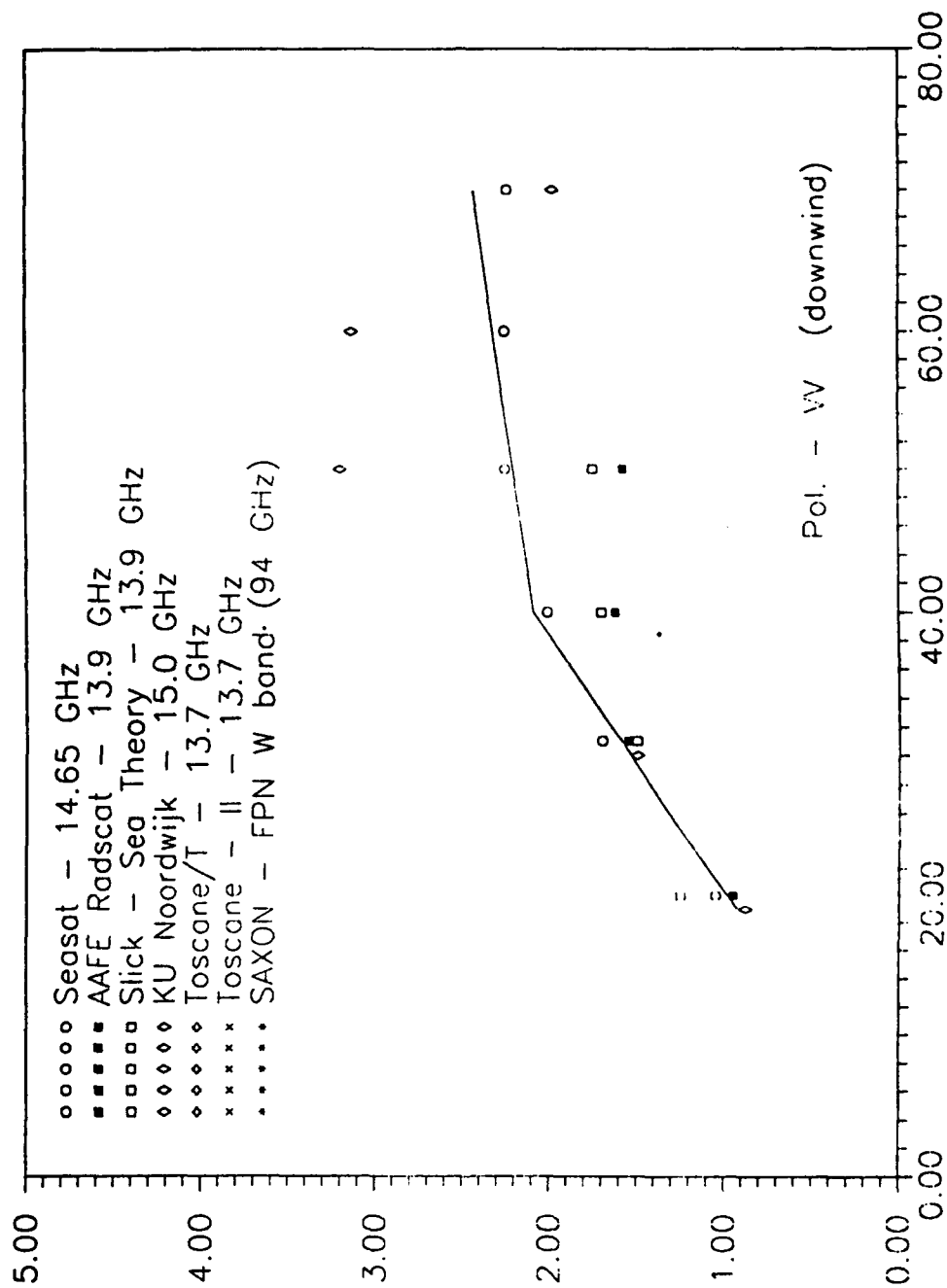


Figure 4-2 Bilinear regression for Downwind under VV polarization.

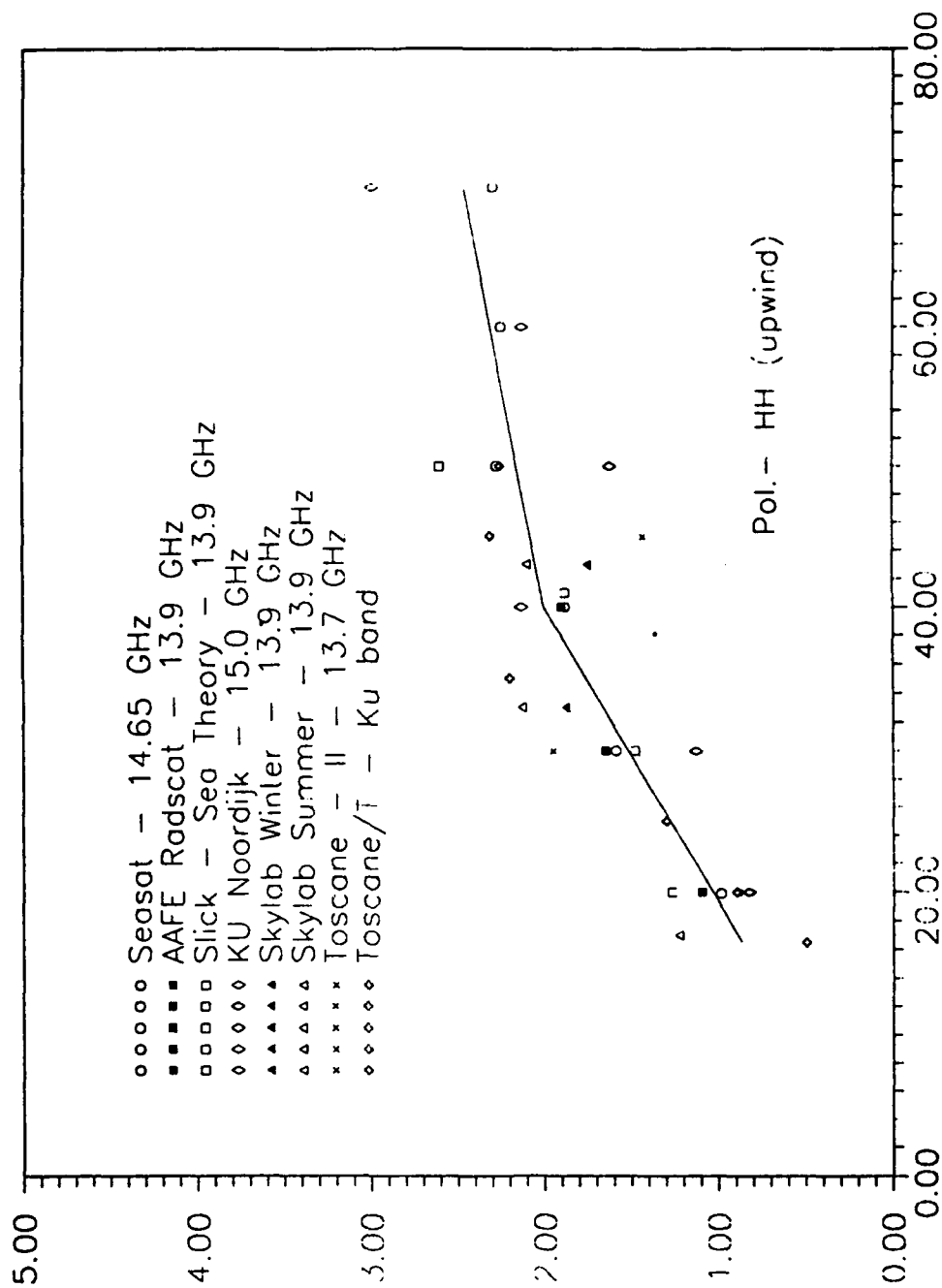


Figure 4-3 Bilinear regression for Upwind under HH polarization.

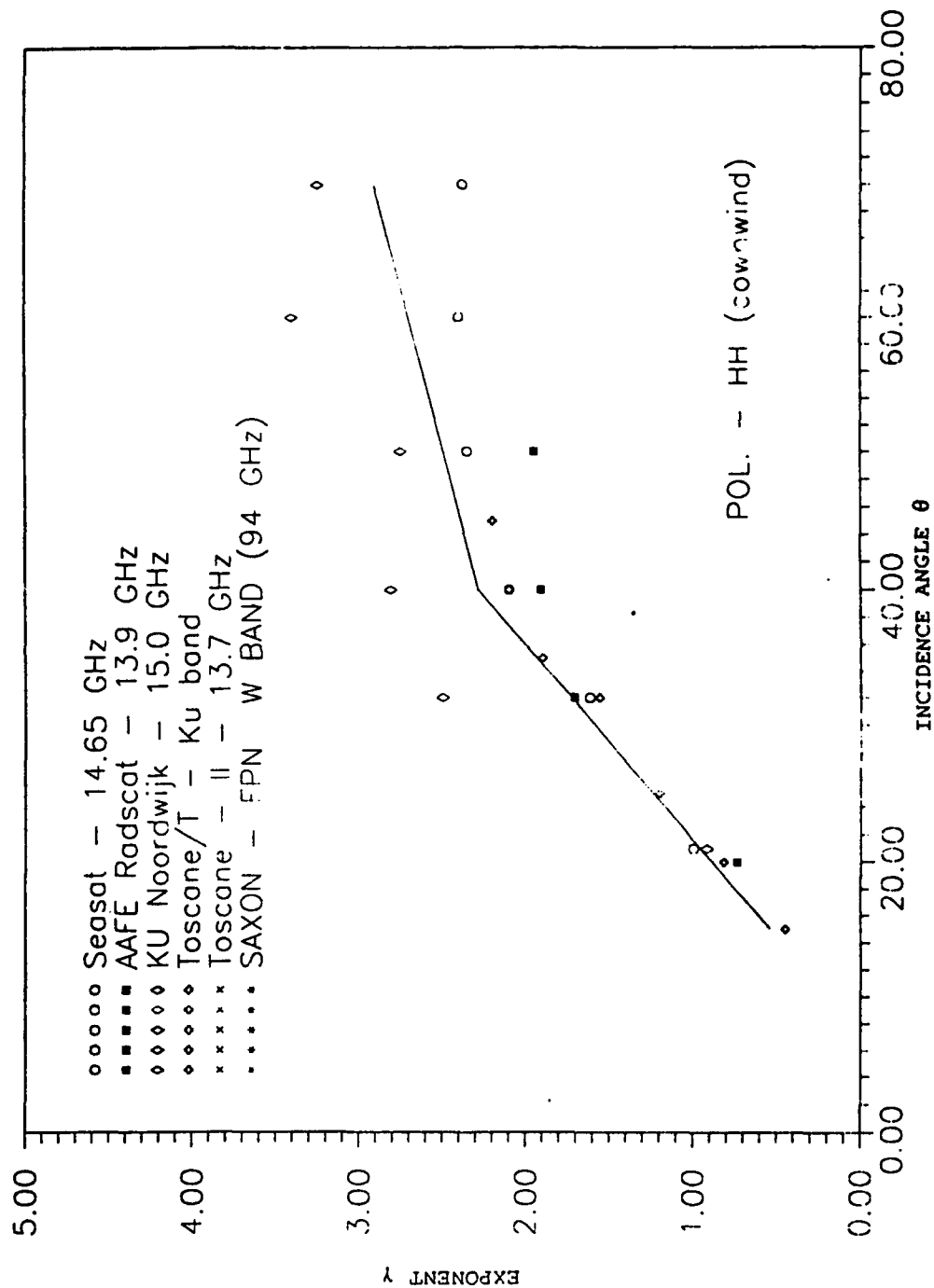


Figure 4-4 Bilinear regression for Downwind under HH polarization.

Table III

Bilinear parameter

INCIDENT ANGLE	$0^\circ\text{---}40^\circ$	$40^\circ\text{---}70^\circ$	$X_b = 40^\circ$
UPWIND-VV	$y_1=0.040x+0.33$	$y_2=0.006x+1.71$	$Y_b = 1.92$
DOWNWIND-VV	$y_1=0.055x-0.13$	$y_2=0.011x+1.64$	$Y_b = 2.09$
UPWIND-HH	$y_1=0.043x+0.07$	$y_2=0.015x+1.39$	$Y_b = 2.00$
DOWNWIND-HH	$y_1=0.070x-0.51$	$y_2=0.021x+1.45$	$Y_b = 2.28$

#### 4-2. Discussion

The experiments summarized here were performed under different conditions. Hence, it is necessary to find optimum values of  $\gamma$  at different incident angles and, through the wind exponent  $\gamma$ , to obtain the ocean surface wind. The bilinear regression plots in Fig.4.1 show, the following:

- (i) The wind exponent  $\gamma$  increases as incidence angle increases for both upwind and downwind.
- (ii) Wind exponent values at Ku band for HH polarization are larger than for VV polarization for incidence angles  $\theta > 20^\circ$ . The difference between them increases with incidence angle.

(iii) The difference of upwind and downwind is obvious after 40°.

(iv) The values from the Seasat experiment (14.65 GHz) and the KU Noordwijk experiment (15.0 GHz), which even are higher than others because KU researchers used the OR method, have very similar values in the bilinear regression equation.



## CHAPTER FIVE

---

### CONCLUSIONS AND SUGGESTION

Wind exponents ( $\gamma$ ) are very important in the study of radar scattering cross-section under ocean-surface conditions. Most experimenters apply the ordinary least-square regression (OLR).

However, OLR accounts for error in only one variable in the regression, and therefore the results of OLR may be not statistically correct. In contrast, the orthogonal regression (OR) provides a good way to estimate two correlation variables ( $x,y$ ) when both of them have errors. The best results are obtained if  $x$  and  $y$  have similar scales.

Our study shows that OR has agreement with OLR when  $x$  is perfectly known without errors. Otherwise, OR and OLR have different results. For example, SAXON-FPN experiment (35 GHz) data demonstrates that orthogonal regression (OR) and ordinary linear regression (OLR) methods have similar wind exponent,  $\gamma$ , if the wave and the wind directions are same. If however, the directions are not the same, the estimates disagree. In this case, the estimate of  $\gamma$  from OR is higher than OLR. It is also seen that  $\gamma$  for cross wind is higher than  $\gamma$  for up wind in both OR and OLR methods. Thus, it is seen that the wind exponent,  $\gamma$ , has a highest value when the wind direction and the wave direction are normal to the radar.

As an important result, when wave direction is similar with wind direction, the slop of the best fit line either in OR or OLR is quite different than that while wave direction is orthogonal wind direction. Therefore, it is obviously to see that the wavedirection is an important factor which

influence the wind exponent  $\gamma$ . These above results may explain some of the scatter of  $\gamma$  values reported in previous experiments. Unfortunately, in most cases, no wave-direction measurements were even made.

Since the 1950s, many experiments on scattering from the ocean have been performed. They give similar but different results for the wind exponent  $\gamma$  that depends on angle of incidence. Wind exponent,  $\gamma$ , appear to vary with angle of incidence in two regions. The data is varied enough that they may be represented by two linear fits. The method of bilinear regression is a simple but obvious way to show the relation between  $\gamma$  and angle of incidence. From the plots shown in Fig.4-1 and Fig.4-2, we can have an idea as to which model function must be used in future experiments, such as EOS. The disadvantage of bilinear regression is that we have to predetermine the vertex point, which can be estimated based only on experience, and there is no particular reason to expect the relation between  $\gamma$  and angle of incidence to be linear.

As bilinear regression important results, the  $\gamma$  values by OR are very identical the bilinear regression equation, such as Seasat data, and the different slopes of upwind and downwind in the bilinear equations are obviously after  $40^\circ$ . Also, the wind exponent  $\gamma$  increases as incidence angle increases for both upwind and downwind, but the slopes for each region are quite different.

As a suggestion for future studies, if enough data are obtained, we may use the OR method instead of the OLR method to specify  $\gamma$  exactly.

#### REFERENCES:

- [1] Moore, R.K., and W.J.Pierson, Jr. "Measuring Sea State and Estimating Surface Winds from a Polar Orbiting Satellite", Proc. Int. Symp. Electromagnetic Sensing of the earth from Satellites, Maimi Beach, FL, Nov. 22-24, pp.R1-R28. (1966).
- [2] MacDonald, F.C. "The Correlation of the Radar Sea Clutter on Vertical and Horizontal Polarization with Wave Height and Slope" IRE Convention Record, Part 1. pp. 29-32. 1956.
- [3] Classen, J.P., R.K.Moore, H.S.Fung, and W.J.Pierson (1972), "Radar Sea Return and the RADSCAT Satellite Anemometer", Proceedings OCEANS'72 IEEE Int Conf. Record pp.180-185
- [4] Ulaby, F.T., R.K. Moore, A.K.Fung, "Microwave Remote Sensing" Vol. iii Ch.20. pp.1647-1790. Artech House, Inc. (1986)
- [5] Moore, R.K.,et al., "Simultaneous active and passive microwave response of the earth -the SKYLAB RADSCAT experiment," Proc. Ninthe Int. Symp. Remote Sensing of Environment Environmental Research Institute of Michigan, Ann Arbor, MI, pp.189-194, Apr. 15, 1974.
- [6] Young, J.D., "Active microwave measurement of sea surface winds from space," Ph.D. dissertation, Univ. of Kansas, Lawrence, Mar. 1976.

- [7] Moore, R.K., J.D. Young, "Active microwave measurement from space of sea-surface winds", IEEE J.Oceanic Eng., vol. OE-2, pp. 309-317, (1977).
  
- [8] Cardone, V.J., W.J. Pierson, Jr., "The measurement of winds over the ocean from SKYLAB with application of measuring and forecasting typhoons and hurricanes," Proc. Eleventh Int. Symp. Space Techniques Sciences (Tokyo, Japan, 1975).
  
- [9] Ross, D., B. Au, W.E. Brown, and J. McFadden, " A remote sensing study of Pacific Hurricane Ava," Proc. Ninth Int. Symp. Remote Sensing of Environment, Environmental Research Institute of Michigan, Ann Arbor, MI, pp. 163-180, Apr. 15-19, 1975.
  
- [10] Jordan, A.K., C.J. Purves, and J.F. Diggs, "An analysis of SKYLAB II S-193 scatterometer data," IEEE Trans. Geosci. Electron., vol GE -14, pp. 97-100, 1976.
  
- [11] Unal, C.M.H., P. Snoeij, and P.J.F. Swart, " The polarization dependent relation between radar backscatter from the ocean surface and surface wind vector at frequencies between 1 and 18 GHz", IEEE Trans. on Geosci. Remote Sensing. Vol. 29. pp.621-626. July 1991.
  
- [12] Daniault, N., " Comparison of sea surface wind measurements obtained from buoy, aircraft and on shore masts during the TOSCANE T campaign", Jour. Atmospheric and Oceanic Technolgh, pp.385-404. June 1988.

- [13] Weissman, D.E., "Dependence of the microwave radar cross section on ocean surface variables: Comparison of measurements and theory using data from the frontal air-sea interaction experiment", Jour. Geo. Res. vol 95, March 15, 1990. pp.3387-3398.
  
- [14] Plant, W.J., "Relating the microwave radar cross section to the sea surface stress: Physics and Algorithms" IGARSS'90 pp.867-871.
  
- [15] Johannessen, J.A, et al. " NORCSEX'88 a pre-launch ERS-1 satellite study of sea imaging capabilities of upper ocean circulation features and wind fronts", IGARSS '90, pp. 707-710.
  
- [16] Onstott, R.G. et al, " scatterometer measurements of wind, waves, and ocean fronts during NORCSEX", IGARSS'90, pp.1094-1088.
  
- [17] Davidson, K.L. and C.E.Skupniewicz, "Wind-stress surface truth measurements for NORCSEX", IEEE Trans. Geos. Remote Sensing, Jan. 1991. pp. 186-189.
  
- [18] Shemdin, O.H., "Tower ocean wave and radar dependence experiment: an overview", J. Geoph. Res. vol.93, Nov. 15, 1988, pp.13,829-13,836
  
- [19] Popstefanja, I., R.E. McIntosh, "Microwave measurements of ocean currents for the SAXON experiment", IGARSS'89, vol.iii. pp.1512-1515.

[20] Gregory, S., "Statistical methods and the geographer," fourth edition, publ. by Lognman, London and New York. 1985.

[21] Bury, K.V., "Statistical Models in Applied Science", publ. by John Wiley & Sons, New York. 1975.

[22] Bain, L.J. and M. Engelhardt," Introduction to probability and mathematical statistics", second edition. publ. by PWS-KENT publishing company. 1992.

[23] Moore, R.K., "A note on weighted orthogonal regression", RSL, The University of Kansas, report for Grant N00014-89-j-3221., December 1992.

[24] Cramer, H., "Mathematical methods of statistics," princeton university press, Princeton, 1946.

[25] Boggs, P.T., & J.E. Rogers, "Orthogonal distance regression," Contemporary Mathematics, 112, pp.183-194. 1990.

[26] Wald, A., "The fitting of straight lines when both variables are subject to error," Annals of Math. Stat., pp. 11,284-11,300.

[27] Vaughan, R.A., "Microwave remote sensing for oceanographic and marine weather-forecast models," Series C:Math. and Physical Sciences, vol. 298. Fig.3, p.107. 1988.

[28] Sistani, B.B., "Measurement and analysis of ocean-radar modulation transfer function at Ka-band (SAXON-FPN experiment)," MS thesis, E&CE Dept. The University of Kansas, 1993.